ST**ET**

Available online at:
stet-review.org

REGULAR ARTICLE

OPEN ◨ ACCESS

Examination of a CI engine running on poppy seed oil biodiesel/n-pentanol/diesel fuel blends with respect of thermodynamic and economic perspectives

Hayri Yaman[1], Gamze Saltan[2], Battal Doğan[2], Murat Kadir Yeşilyurt[3,*] (iD), and Selçuk Sarıkoç[4]

[1] Kırıkkale University, Department of Automotive Technology, Kırıkkale, 71450, Türkiye
[2] Gazi University, Department of Energy Systems Engineering, Ankara, 06560, Türkiye
[3] Yozgat Bozok University, Department of Mechanical Engineering, Yozgat, 66200, Türkiye
[4] Amasya University, Department of Mechanical Engineering, Amasya, 05100, Türkiye

Abstract. The present study regards thermodynamic and economic analyses of a compression-ignition engine running on various blends of biodiesel, n-pentanol, and diesel at different ratios. Diesel fuel and n-pentanol were obtained from commercial companies while biodiesel was produced from poppy (*Papaver somniferum* L.) seed oil by transesterification method under laboratory conditions. Five fuel blends (diesel fuel, B30Pt30, B30Pt20, B30Pt10, and B30) prepared in different ratios by volume were used in the experimental process. Engine tests were performed at a stable speed (1500 rpm) and four different loads from 25% to 100%. Engine performance data from the dynamometer and harmful emissions from the exhaust emission device were determined. These data were used in energy, exergy, and economic analysis. The energy analysis determines how much of the fuel's energy was spent on generating power from the crankshaft and thermal losses. In addition, the fuel inlet exergy, exhaust exergy, exergy of thermal losses, and exergy destruction were found throughout the exergy analysis, meanwhile, exergoeconomic analysis was conducted to understand the cost of the energy absorbed and losses at the crankshaft. At maximum engine load, energy efficiency was acquired to be between 25.99% and 34.63% and exergy efficiency between 28.87 and 32.34% as a consequence of the use of test fuels in the diesel engine. The higher cost of the work taken from the crankshaft in binary and ternary fuel blends in the study is on account of the high pump prices of biodiesel and n-pentanol compared to conventional diesel. At 100% load, the cost of the work noted from the crankshaft for diesel fuel, B30, B30Pt10, B30Pt20, and B30Pt30 fuels is 211.86, 2126.77, 3001.27, 3755.02, and 3755.02 \$/GJ, respectively.

Keywords: CI engine, Thermal efficiency, Exergy, Exergoeconomic, Sustainability index.

Nomenclature

$\dot{C}$ (\$/h)	Cost rate of exergy flow
c (\$/kJ)	Specific cost
C_p (kJ/kg K)	Specific heat capacity
E (kW)	Energy flow
$\dot{Ex}$ (kW)	Exergy flow
f (−)	Exergoeconomic factor
H_u (kJ/kg)	Lower heating value
H (kJ)	Enthalpy
$\dot{m}$ (kg/s)	Mass flow rate
N (year)	Lifetime
P (kPa)	Pressure

$\dot{Q}$ (kW)	Heat transfer rate
r_c (−)	Relative cost difference
rpm	Revolutions per minute
S (kW/K)	Entropy
SI (−)	Sustainability index
$\overline{R}$ (J mol/K)	Gas constant
T (K)	Temperature
y^e (%)	Component mole fraction
$\dot{W}$ (kW)	Work

Abbreviations

BSFC	Brake specific fuel consumption
BTE	Brake thermal efficiency

* Corresponding author: kadir.yesilyurt@bozok.edu.tr

B20	80% diesel + 20% biodiesel
B30	70% diesel + 30% biodiesel
B100	100% biodiesel
B30Pt10	60% diesel + 30% biodiesel + 10% n-pentanol
B30Pt20	50% diesel + 30% biodiesel + 20% n-pentanol
B30Pt30	40% diesel + 30% biodiesel + 30% n-pentanol
bTDC	Before top dead center
CI	Compression-ignition
CO_2	Carbon dioxide
CO	Carbon monoxide
DF	Diesel fuel
ECI	Environmental cost indicator
EEI	Energy efficiency index
HC	Unburned hydrocarbon
HCCI	Homogeneous-charge compression-ignition
HDH	Humidification-dehumidification
ICE	Internal combustion engine
LPG	Liquefied petroleum gas
NO_X	Oxides of nitrogen
NPV	Net present value
O_2	Oxygen
PM	Particulate matter
PPME	Pongamia pinata methyl ester
PSOB	Poppy seed oil biodiesel
PTO	Power take-off
RCCI	Reactivity-controlled compression-ignition
SCUP	Sum unit cost of product
SEM	Scanning electron microscopy
SI	Spark-ignition
SPECO	Specific exergy costing

Subscripts

0	Environmental conditions
a	Air
chem	Chemical
cw	Cooling water
dest	Destruction
ex	Exhaust
f	Fuel
gen	Generation
heat	Heat transfer
in	Inlet
out	Outlet

Greek symbols

η	Thermal efficiency
η_{II}	Exergy efficiency
φ	Fuel exergy factor
ε	Exergy flow
μ	Gas viscosity

1 Introduction

The energy requirement of the world has been rapidly growing as population and economic growth increase day by day. Between 2012 and 2040, there was a 48% energy growth. This growth also increases the use of fossil-based fuels. More than 80% of global energy consumption today comes from fossil-based resources such as coal, oil, and natural gas. In addition, fossil-based fuels are projected to satisfy about three-quarters of total energy demand in 2040. On the other hand, the widespread use of traditional fuels, particularly in the transportation sector, has resulted in considerable health problems and environmental hazards. Combustion products in fossil fuels cause atmospheric pollution and various environmental problems like global warming. To overcome the challenges posed by fossil fuels, the shift towards renewable and alternative energy sources is increasing more than ever. Therefore, there is growing interested in the advancement of eco-benign renewable, clean, and sustainable fuel types like biomethanol, bioethanol, and biodiesel and to comparatively take the place of their fossil-driven counterparts [1, 2].

Compression-Ignition (CI) engines have been widely preferred in transportation, agriculture, power generation, and many other areas for their better characteristics as follows: durability and elevated torque capacity. CI engines running on fossil-derived Diesel Fuel (DF) cause high soot and oxides of nitrogen (NO_X) emissions that pose serious environmental and health issues. In this sense, researchers have been looking for clean and affordable alternative fuels [3].

The eco-friendly and renewable fuels in liquid form, which are among the biofuels produced from new or used vegetative oils, algae, and animal oils by chemical methods, are called biodiesel. Biodiesel can be defined as an energy-efficient, clean, sustainable, renewable, biodegradable, and sulfur-free fuel. Biodiesel displays similarities to petroleum diesel fuels in the context of physical and chemical characteristics. For that reason, this alternative energy source is potentially utilized in existing CI engines. Regardless, it shows lower performance than the DF operation. Biodiesel has different combustion behaviors in comparison with conventional DF. For that reason, it needs analysis from distinct perspectives to fully assess its usefulness as an alternating fuel for CI engine applications. The physicochemical specifications of biodiesel are important for the purpose of understanding the engine performance and harmful pollutants [2]. Biodiesel can be synthesized from oil-bearing crops such as soybean, hemp, mustard, canola, safflower, peanut, sesame, cottonseed, rubber, and sunflower, or animal fats such as fish, chicken fat, and beef tallow. Biodiesel is the methyl or ethyl ester of vegetable oils and it is the most appreciated kind of sustainable and renewable alternative fuel. Pure biodiesel and biodiesel/DF binary mixtures can be appreciated in specific fractions in a CI engine without any major modifications [4].

Alcohols such as methanol-C1, ethanol-C2, propanol-C3, butanol-C4, pentanol-C5, and gaseous fuels such as Liquefied Petroleum Gas (LPG) have been embraced as alternative fuels instead of fossil fuels in Internal Combustion Engines (ICEs). Alcohol-based fuels can be employed in ICEs in pure form or as a blend with fossil fuels [5].

Alcohols have a higher oxygen content in their molecular structure than those of DF and biodiesel. On the grounds of the aforementioned characteristics, the alcohols provide better combustion, provide high heating, give lesser NO_X emissions, and do not cause corrosion [6]. Ethanol can be produced from any source that contains sugar. Ethanol is a widely used biofuel as it is appropriate for use in both CI and Spark-Ignition (SI) engines. Ethanol can be the best blend when used with DF. When mixed with DF, there is an increment in ignition rate and enhancement in the combustion reaction. Therefore, blended ethanol significantly increases engine efficiency. The biggest variation between DF and alcohol-based fuels is the oxygen content. When the CI engines operate with an oxygenated fuel, reduction has been observed in the carbon monoxide (CO), smoke, and unburned hydrocarbon (HC) emissions. Advanced ICEs, such as Homogeneous-Charge Compression-Ignition (HCCI) engines, have benefited in overcoming the limitation of high CO and HC emissions. However, pure ethanol is not widely used owing to poor auto-ignition quality and converting a CI engine into a SI engine [7, 8]. The open formula of methanol is CH_3OH. It is a colorless, odorless, and poisonous alcohol. It is flammable and burns with an invisible flame. Improvements are constantly being made to the synthesis of methanol. It is to be noted that methanol can be attained in many ways. It may be, for instance, acquired from biomass, coke oven gas, or natural gas. In continuous production, it can be recovered by flash evaporation. Consequently, methanol can also be employed in high-compression ratio SI engines that can replace DFs [9].

There are concerns about the suitability of food-grade vegetable oils considered in the production of biodiesel due to human consumption. Accordingly, in-edible vegetable oils and waste frying oils can be contemplated in the production of biodiesel. On the other side, the case that alcohols (methanol, ethanol, etc.) have phase separation problems at low temperatures when evaluated in the fuel blends, and the high repair costs of CI engines prevent the use of alcohols. Alcohols also have low engine performance. Because of some shortages, it has been recommended to utilize higher-order alcohols that have fuel characteristics such as high energy content, high cetane number, and lesser latent heat of vaporization. The main higher carbon alcohols are propanol-C_3H_7OH, butanol-C_4H_9OH, and pentanol-$C_5H_{11}OH$. The aforementioned alcohols can be conveniently mixed with both biodiesel and DFs at desired concentrations without any phase separation issues. Besides that recent high-capacity production technologies have enabled a depletion in the cost of producing pentanol in contrast to butanol [10]. It is extremely remarkable as a means to examine the influence of higher carbon alcohol on engine performance, harmful pollutants, and combustion behaviors of the CI engine operating with DF, biodiesel, or DF/biodiesel blends [11].

As is well-known, the exergoeconomic concept is a technique commenced in the 1930s and used to design functioning energy conversion systems or to optimize such systems. It evaluates the economy along with the 2nd law of thermodynamics via economic and exergy perspectives [12].

There are thermodynamic analysis studies on alternative fuels for CI engines in the literature. Some of these studies are presented in summary. Ding *et al.* [13], for instance, aimed to recover waste heat in their study. The researchers proposed to use cogeneration of electrical energy and freshwater for the recovery of waste energy from a CI engine. The Kalina cycle used in the study utilizes the Humidification-DeHumidification (HDH) technique in order to generate power and production of freshwater by using waste energy. Optimization, thermodynamic, and exergoeconomic analyses were performed in this intended system. The influence of the factors on HDH unit performance, exergy efficiency, net output power, and total unit cost of the system product was investigated in detail. An assessment of the optimization outcomes with the fundamental case results showed that thermal and exergy efficiency values were raised by 1.88 and 1.52%, respectively. The researchers estimated the payback period as 7.2 years for an electricity selling price of 0.09 $/kWh. In addition, it was calculated that the Net Present Value (NPV) of the plant was to be $165,814 at the end of its lifetime. In their study, Shelar and Kulkarni [14] recommended a trigeneration system to utilize energy from water circulating in the engine jacket and exhaust gases for cooling loads thanks to absorption chiller equipment. An engine-based trigeneration system having a thermal stabilizer was proposed to be integrated with an auxiliary or compression chiller system. The comparison of the two options is tested based on thermodynamics and annual life cycle cost for a typical hotel. Trigeneration systems with compression chillers are found to be more effective than trigeneration systems without compression chillers in the case of a hotel settled in the inner peninsular region of India. Interestingly, Mao *et al.* [15] aimed to design the cogeneration of electricity and fresh water to recover the waste energy from a CI engine. It could be reported that the conversion of waste energy from CI engines into beneficial work and engine improvements would enhance thermal management strategies and efficiency. It utilized a dual-pressure Kalina cycle and HDH desalination system for freshwater production and generation of power by means of jacket water energy and exhaust gas energy, respectively. The researchers also applied thermodynamic and economic analyses to model the proposed system. The practicability of the plant for investment was taken into consideration using the concepts of payback period and NPV. According to the outcomes, it could be obtained that the maximum exergy destruction value was notified to be 39.88 kW for the condenser, meanwhile, the payback period and NPV findings were computed to be $165,814 and 7.4 years, respectively, considering the electricity price of 0.09 $/kWh. In their study, Çetin and Sogut [16] first developed an energy efficiency strategy framework to support efficient energy management as a decision-support element in ships. Energy efficiency and economic efficiency, exergy approach, and economic criteria have been analyzed by considering the ship's navigation processes. In this framework, two novel criteria "Environmental Cost Indicator (ECI)" and "Energy Efficiency Index (EEI)" were in proposed to the recent literature. Based on the results of the present analyses, the

energetic and exergetic efficiency values of the ship in the navigation processes were computed to be 38.33% and 35.82%, respectively, and the ECI was deciphered to be 0.41. With the abovementioned acknowledged values, the fuel-related lost cost of the ship was found to be 19.05%. To conclude, some considerable evaluations of the application and effects of the energy efficiency strategy were comprehensively made. Cavalcanti [17] investigated the gas DF-fueled marine engines operated for trigeneration systems with respect to thermodynamic and exergoenvironmental perspectives. The manufacturers of marine engines have explained the development of a dual-fuel mode version to enhance the combustion process and decrease pollutant gas emissions. The objective of the study was to evaluate the performance of gaseous DF and normal DF mode according to exergy and exergoenvironmental concepts. The researcher applied a SPecific Exergy Costing (SPECO) approach using fuel and product definition. The original diesel marine engine generated 6.90 MW of electric power, 28.16 kW of cooling water, 278.2 kW and 588 kW of heating. According to the findings, gas DF declined the energy and exergy efficiency values by 87% in comparison with full DF mode. It was calculated that the CI engine has the highest exergy destruction rate with 3051 kW. Electric power, absorption chiller cooling water, and heating water presented an environmental impact ratio per exergy unit. In spite of the reduction in energetic and exergetic efficiency, dual-fuel mode technology reduced pollutants and enhanced external environmental performance without major modifications to the engine. Krishnamoorthia et al. [18], examined the results coming from the infusion of syngas and biodiesel for a diesel-fueled Reactivity-Controlled Compression-Ignition (RCCI) engine. Scanning Electron Microscopy (SEM) of exhaust Particulate Matter (PM) was taken into account with a focus on comprehending the morphology of PM. Energy and exergy analyses were performed to acquire energy and availability shares and to guide energy recovery systems. In the aforementioned study, they investigated the effect of injection parameters on compression in a CI engine fueled by synthesis gas, DF, and B20 (80% DF+20% biodiesel). The researchers studied the optimum operating conditions for syngas/B20 and syngas/DF in RCCI mode for several working parameters. In this sense, the injection timing, pre-injection mass, and fraction injection pressure were changed for the purpose of achieving enhanced combustion efficiency at medium load. It could be reported that the syngas/DF mode operation with the injection timing of 19° before Top Dead Center (bTDC) showed 77% and 22% lesser PM and NO_X emissions, respectively, and slightly higher Brake Thermal Efficiency (BTE) as compared to conventional DF. Furthermore, SEM results demonstrated that the number of fine particulate (PM < 2.5 μm) emissions descended in syngas/B20 and syngas/DF dual-fuel mode combustion. The exergy analysis indicated that for most operating conditions, the destroyed availability was lesser at 80% load compared to 62% load. Hosseinzadeh-Bandbafha et al. [19] intended to analyze a heavy-duty tractor CI engine fueled with the ternary blends of bioethanol, biodiesel, and DF with regard to exergy, economic, and environmental

assessment. On this basis, traditional DF was blended with bioethanol and biodiesel at volumetric ratios of 2–6% and 5–15%, respectively. Hence, nine dissimilar kinds of bioethanol, biodiesel, and DF blends were performed at various power take-off (PTO) shaft speeds varying between 800 and 1000 rpm under full-load operating conditions. Several indicators such as exergetic, economic, and environmental were taken into account so as to achieve decision-making on the composition of the fuel and PTO shaft speed. The researchers highlighted that the PTO shaft power generation cost and weighted environmental impact of the chosen fuel blend were 46.2% and 44.3% less than that of DF mode operation, respectively. In addition, the environmental sustainability and resource employment efficiency of the selected fuel blend were observed to be 99.8% and 97.3% higher than that of DF, respectively. Zhu et al. [20] studied a new steam-jet turbo-compound system to recover waste energy from a two-stroke CI engine. Initially, the researchers built a sophisticated thermodynamic model according to energy and exergy analysis, integrating an overhead in-cylinder diesel cycle and a bottom steam injection Brayton cycle. This was compared with the base engine and they reported that fuel consumption can be reduced by 5.1% at nominal speed with the new steam injection turbocharger. With the conventional turbocharger, they found that the improvement rate was around 3.3%. In conclusion, it could be reported that the aforementioned new steam injection turbocharger system displayed better fuel economy performance than that of conventional systems. Vandani et al. [21] studied the combined cycle power plants. It was stated that the energy consumption of combined cycle power plants was high. Besides that, the researchers investigated the influence of using DF instead of natural gas for a power plant in Iran in a view to exergy, economic, and environmental impacts. Consequently, the exergy efficiency of the plant operating with natural gas as fuel was calculated to be 43.11%. The exergy efficiency of the DF and natural gas plants was computed to be 42.03% and 43.11%, respectively. Economically, the price of natural gas was cheaper than DF; for that reason, the fuel cost was lower. Nabi et al. [22] studied the main factors causing diesel NO_X formation and evaluated energy and exergy factors using e-diesel blends. They investigated the main factors affecting the formation of diesel NO_X ethanol-diesel (e-diesel) blends. It was to noted that cylinder pressure was directly proportional to experimental in-cylinder pressure data simulated with GT-Power and ANSYS data. Among the four fuels, all three blends showed less NO_X than pure DF. The oxygen content and energy and exergy parameters showed insignificant differences between the four fuels. Khoobbakht et al. [23] tested DF-biodiesel-ethanol blend fuels in a direct-injection CI engine. The researchers calculated the operating factors of load and speed. They also studied the effect of biodiesel and ethanol on the exergetic efficiency of DF blends. They used the first and second laws of thermodynamics to analyze energy and exergy parameters. As a result, they figured out that the exergy efficiency decreases with the augmentation percentage by volume of biodiesel and ethanol fuel. In their study, Paul et al. [24] aimed to analyze a CI engine subjected to a mixture of Pongamia Pinata Methyl Ester (PPME) and

DF-ethanol blends. PPME concentration was kept at 50%. The ethanol percentage ranged from 5 to 20% in 5% intervals. DF contribution was reduced. They conducted a detailed analysis of exergy, combustion, emissions, and efficiency. It was concluded that the D35E15B50 blend had the best engine performance with a 21.17% increase in BTE and a 4.61% decrease in brake energy consumption. When they performed the exergy analysis, they found that there was a 25.64% increase in exergy efficiency at full load for the D35E15B50 blend. In addition, the exergy analysis showed that the addition of ethanol to DF-biodiesel blends at a concentration of up to 15% (by volume) can reduce losses and improve energy utilization in the engine. In their study, Costa et al. [25] operated a CI engine with two fuels (natural gas and DF). They performed theoretical and experimental studies and calculations while the engine was running. The experimental plant (thermal system) they studied consists of a CI engine connected to an electronic generator with measurement sensors for pressure, temperature, air, natural gas, DF flow meters, gas analyzer, gas converters, and power intake system, consisting of an electrical load. In this study, the CI engine was operated at powers ranging from 10 to 150 kW and with replacement ratios between 60% and 85%. When the engine was operated with pure DF, the total exergy varied from 85 to 425 kW. When the engine was operated as a duo (natural gas and DF), the total exergy of the engine varied between 131.0 and 287.3 kW. Taghavifar et al. [26] replaced renewable fuels containing methanol and dimethyl ether blends with DF at different percentages using an HCCI engine. They conducted numerical research on this study. They found that D80, which has the highest proportion of DF in its composition (80%), has the worst energetic and exergetic performance among the blends. Cavalcanti et al. [27] performed exergy, exergoeconomic, and exergoenvironmental analyses of a stationary, direct-injection CI engine to verify the influence of engine load and biodiesel proportion. The analysis included calculations such as exergy efficiency, specific environmental impacts, specific cost, exergoenvironmental and exergoeconomic impact indicators. In their analysis, they obtained the best results at full-load operation. As a result of the exergy analysis, they found that lower biodiesel concentration gives higher efficiency. They found that the exergoeconomic factor mitigates as a consequence of the increase in exergy destruction and exergy losses. Zapata-Mina et al. [7] calculated the results of exergy analysis at different operating conditions in a single-cylinder CI engine with different compression ratios operated with DF, ethanol, and gasoline/ethanol blends. The results of the experimental study conditions of the modified engine, operating at a 12:1 compression ratio of 50% and ethanol blend, computed that it performs better in terms of exergetic efficiency and environmental impact factor. Aghbashlo et al. [28] aimed to determine the exergy of a single-cylinder direct-injection CI engine by adding various fuel blends. The engine is at a constant speed of 1000 rpm. 95% DF + 5% biodiesel blend (B5) (3%, 5%, and 7%) was diluted with water, and engine tests were performed at four engine loads (25–100%). The findings presented that load and fuel type affect the exergy efficiency of the engine. They found that increasing engine load

reduces the exergy efficiency. Among the prepared fuels, the mixture of 3% water and B5 showed the best exergy efficiency at all engine loads investigated. Suresh et al. [29] investigated the influence of biodiesel obtained from waste cotton oil on engine performance and exhaust emissions. Their test results showed that biodiesel decreases thermal efficiency, low biodiesel content decreases Brake Specific Fuel Consumption (BSFC) and mitigates CO and HC emissions while increasing NO emissions. They also stated that the addition of biodiesel to DF augments the maximum cylinder pressure values. In their comparative study on the effect of physicochemical properties of biodiesel synthesized from edible and non-edible oils on biodiesel blends, Atabani et al. [30] reported that biodiesel blends can be improved relying on the feedstock source used and the related blend properties can be predicted by polynomial curve fitting method. Atabani et al. [31] also evaluated in detail the raw material source, extraction, properties and quality, production methods, problems and potential solutions of vegetable oil utilization, advantages and disadvantages, economic viability and sustainability of biodiesel, and its future. Feedstock accounted for about 75% of the cost in the entire biodiesel production process. Therefore, they demonstrated the importance of choosing the best feedstock source for the lowest production cost. In addition, they stated that biodiesel is used more effectively as a complement to other energy sources. Çengelci et al. [32] tested biodiesel produced from animal (tallow) and vegetable (poppy oil) oils in a single-cylinder, four-stroke, direct-injection, Antor 3 LD 510 CI engine and compared engine performance and harmful pollutants with DF. As a result, they found that when animal fat-based biodiesel was used, torque and effective power values declined, BSFC ascended and CO emission descended in terms of engine performance characteristics compared to DF. They determined that when vegetable oil-based biodiesel was used, BSFC, engine torque, and engine power improved, exhaust gas temperatures increased, carbon dioxide (CO_2) emissions increased, and smoke darkness diminished compared to DF. Eliçin et al. [33] researched biodiesels produced from hazelnut, poppy, sunflower, canola, corn, cotton, soybean, and olive oils in a single-cylinder, 5.5 kW Lombardini LDA 450 CI engine and investigated engine performance and exhaust emissions in comparison with DF. As a result, they concluded that with the use of biodiesel, engine torque, and power decreased, BSFC increased, HC and CO_2 emissions decreased, while CO and NO_X emissions boosted compared to DF. Another considerable research was conducted by Imdadul et al. [34], who added biodiesel, synthesized from tamanu oil via transesterification reaction, and pentanol to DF at 10%, 15%, and 20% and compared performance and emission parameters with B20 binary blend when the tested fuels were experimented in a single-cylinder, 8.8 kW, water-cooled, TF 120 M CI engine. In conclusion, they found that thermal efficiency increased by 15%, BSFC reduced by 8.7%, engine power ascended by 10.4%, NO emission increased by 4.4%, whereas HC, smoke, CO_2, and CO emissions diminished by 43.45%, 21.2%, 2.5%, and 33.1%, respectively. The researchers also marked that the infusion of pentanol increased the maximum in-cylinder

pressure, enhanced combustion, and postponed the onset of the combustion reaction. Zhu *et al.* [35] infused n-pentanol to waste cooking oil biodiesel at 10%, 20%, and 30% (by volume) and tested in a four-cylinder, water-cooled CI engine and compared their combustion and exhaust emission characteristics with DF. Finally, they observed that with the augmentation in the n-pentanol content in blended fuels, the crank angle at which the start of combustion and maximum heat release occurred moved away from the top dead center, and the cylinder pressure and heat release rate were enhanced. The researchers indicated that HC and CO emissions augmented with the utilization of blended fuels compared to DF and biodiesel, and NO_X emissions mitigated compared to biodiesel up to 20% alcohol blend.

The use of biodiesel and alcohols as alternating fuels in CI engines is a topic worthy of research due to diminishing fossil fuel resources and environmental problems. When the studies in the literature are examined, there are generally experimental performance and emission studies on DF, biodiesel, and alcohol. In this study, unlike other studies in the literature, economic evaluations were carried out through thermodynamic analyses using performance and emission data of biodiesel and alcohols. In this study, energy dissipation, exergy efficiency, exergy efficiency, exergy dissipated, and the cost of power taken from the crankshaft were investigated in five different fuel blends by thermodynamic analysis.

2 Material and method

This section presents comprehensive knowledge regarding test fuel preparation, engine set-up, and analyses.

2.1 Test fuels

In this study, poppy (*Papaver somniferum* L.) seed oil was used as a feedstock for biodiesel fuel production. Petroleum-derived DF was procured from a local gas station in Yozgat. The relevant company explained that the DF properties meet EN 590 standards. Transesterification reaction, which is the most preferred method in the literature, was preferred for biodiesel production. In the transesterification reaction, methanol with ≥99.9% purity value as alcohol and NaOH pellets with ≥99.5% purity value as catalyst were used. Methanol was purchased from *Carlo Erba Reagents* (France), and the catalyst was from *Chemsolute a brand of Th. Geyer* (Germany). The oxygenated fuel additive used in the preparation of blended fuels was n-pentanol purchased from *Merck* (Germany) with a molecular weight of 88.15 g/mol, purity ≥99%, and 18.18 wt.% oxygen in its chemical structure. Long-chain alcohols from renewable sources have better fuel properties and are a better option than lower-chain alcohols when compared to blended fuels. n-pentanol has a five-carbon chain. It is a type of alcohol that can be easily blended with DF and biodiesel [10]. Poppy Seed Oil Biodiesel (PSOB) production was carried out under a 9:1 methanol-oil molar ratio, 0.75 wt.% NaOH, 60 °C reaction temperature, and 60 min reaction time.

A detailed description of the above-mentioned reconstitution conditions and biodiesel production is presented in reference [36]. After PSOB production, PSOB-DF binary blend and PSOB-DF-alcohol ternary blends were prepared. In the first stage, PSOB and DF were blended by volume (30–70% by vol.). Then, n-pentanol was added to the prepared binary mixture at ratios of 10%, 20%, and 30% with a PSOB ratio of 30%. In conclusion, one binary blend (B30) and 3 ternary blends (B30Pt10, B30Pt20, and B30Pt30) were prepared. The test fuels were kept in sealed bottles at room temperature and in the dark for 7 days. Phase separation did not occur in any of the fuel mixtures. However, all fuels were homogenized by shaking again before the engine tests. The physicochemical properties of the tested fuels used in the study are tabulated in Table 1. Kay's mixing rule − $\varphi_{\mathrm{mix}} = \sum_i^n x_i \cdot \varphi_i$ equation was implemented to determine some of the physicochemical specifications of the blended fuels [37].

As observed from Table 1, DF has the lowest density. When the carbon percentages are examined, it is seen that DF has a higher percentage of carbon by weight. As the carbon percentage increases, the energy capacity of the fuel will ascend more. The energy content is the amount of heat released during fuel combustion. If standard conditions are met, this indicates the total amount of energy released as heat when fully combusted with oxygen [9]. Table 1 shows DF as having the highest calorific value.

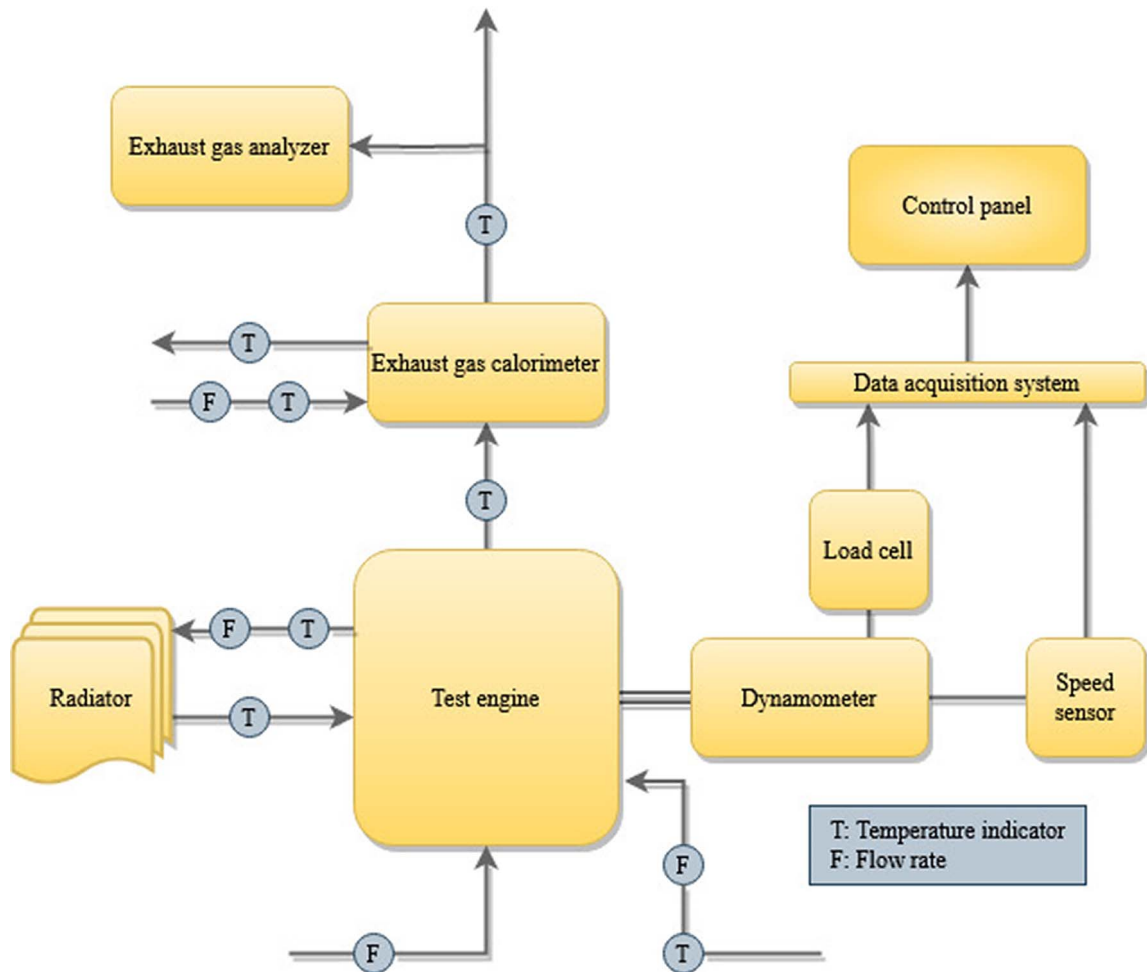### 2.2 Engine test setup and experiments

Engine experiments were carried out at *Kırıkkale University Automotive Technology Program Engines Laboratory*. The test engine is a single-cylinder, four-stroke, water-cooled, direct-injection CI engine. The experiments were conducted at a constant speed and several loads. A schematic view of the engine test rig is plotted in Figure 1. Bilsa brand MOD 2210 model exhaust gas analyzer was used for the measurement of exhaust emissions. The technical specifications of the test engine and the measurement equipment used in the experimental setup are given in Table 2 and Supplementary file in detail, respectively.

Before starting the engine experiments, the devices used in the experiments were checked and calibrated. The engine was started slowly, and the engine running-in period was completed and the stable operating conditions of the engine were determined by performing preliminary experiments. In order to determine the stable operating conditions of the engine, changes in the engine oil temperature, exhaust gas temperature, and engine cooling water temperature were observed. The engine was determined to reach stable operating conditions approximately 15–20 min after the engine was started at idle. Before starting the engine experiments, all problems encountered in the preliminary tests of the engine test system were eliminated and the actual experiments were started. All experiments were carried out after the engine had reached full operating temperature and stabilized. The test engine is operated at 1500 rpm at the value specified by the manufacturer. Therefore, in the engine experiments, engine performance and emission characteristics were investigated for each test fuel separately at

Table 1. Physicochemical specifications of tested fuels [36, 38–41].

Property	Unit	DF	PSOB	n-pentanol	B30	B30Pt10	B30Pt20	B30Pt30
Chemical formula	–	$C_{14}H_{25}$	$C_{17.41}H_{11.62}O_2$	$C_5H_{12}O$	–	–	–	–
Carbon	wt.%	87.05	76.64	68.18	83.93	82.04	80.15	78.27
Hydrogen	wt.%	12.95	11.62	13.64	12.55	12.62	12.69	12.76
Oxygen	wt.%	–	11.74	18.18	3.52	5.34	7.16	8.98
Carbon/Hydrogen	–	6.722	6.596	4.632	6.687	6.501	6.317	6.135
Density	kg/m^3	830	884	814	846.20	844.60	843.00	841.40
Energy content	MJ/kg	42.80	39.08	36.10	41.68	41.01	40.34	39.67
Cetane number	–	55	41.51	17	50.95	47.15	43.35	39.55
Copper strip corrosion*	Degree of corrosion	1a	1a	–	–	–	–	–
Flash point	°C	60	>120	49	–	–	–	–
Water content	ppm		<500					
Latent heat vaporization	kJ/kg	250	–	308	–	–	–	–

* 3 h at 50 °C.

Fig. 1. Schematic representation of the test setup.

Table 2. Technical specifications of the test engine.

Test engine	
Items	Specifications
Brand-Model	Kirloskar-TV1
Ignition	Compression-ignition
Engine speed	1500 rpm
Cylinder number	1
Stroke number	4
Cooling system	Water-cooled
Maximum power	5.2 kW
Aspiration	Naturally-aspirated
Bore × Stroke	87.50 mm × 110.00 mm
Displacement	661.45 cc
Fuel injection timing	23° bTDC
Nozzle opening pressure	200 bar
Fuel type	Multi-fuel
Compression ratios	12:1–18:1
Fuel tank capacity	15 L
Intake valve closing delay	35.5° aBDC
Intake valve opening advance	4.5° bTDC
Exhaust valve closing delay	4.5° aTDC
Exhaust valve opening advance	35.5° bBDC
Fuel injection type	Direct-injection
Injector	Denso
Connecting rod length	234 mm

a constant speed (1500 rpm under four different engine load operating conditions: full load (100%), three-quarters load (75%), half load (50%), and quarter load (25%). The aforementioned values represent the engine load conditions of 15, 11, 7.4, and 3.7 kg, respectively. During the experiments, the environmental conditions were measured as atmospheric temperature $T_0 = 25$ °C and relative humidity between 40% and 50%. However, the experiments were repeated three times, and calculations were made with the average of the results obtained. The experimental procedure described in this section was repeated for all fuel samples and the effects of alternative fuels on engine performance and pollutant emissions were determined. Thermodynamic and economic analyses were accomplished using the data recorded.
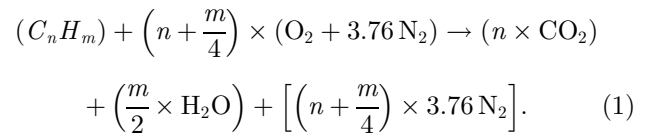
3 Thermodynamic analysis

First law of thermodynamics expresses the conservation and transformation of energy. First law states that energy cannot be created out of anything. Energy can only transform into another form of energy. Second law of thermodynamics states that energy has a quality and that the quality of energy will decrease during changes of state. To better understand ICEs, energy, and exergy analysis should be applied together [42].

Figure 3 shows a schematic representation of the control volume used in the thermodynamic analysis. The energies

entering the control volume are the energy from the chemical energy of the fuel and the energy from the incoming air. The energy of the fuel and air entering the engine is used to generate power from the crankshaft. Thermal losses occur during power generation. These thermal losses are heat transfer from the engine body, energy transferred to the cooling water, and exhaust energy. Apart from these, friction, uncontrolled combustion, etc. losses are not included in the calculations but are shown as other total losses. Since the temperature and pressure of the incoming air are the same as the dead ambient conditions, the energy of the incoming air is equal to zero. Therefore, the energy of the incoming air is considered zero in energy and exergy calculations [43].

After the complete combustion of fuel and water, CO_2, and nitrogen are emitted. It is formulated as shown in equation (1):

$$(C_nH_m) + \left(n + \frac{m}{4}\right) \times (O_2 + 3.76\,N_2) \rightarrow (n \times CO_2)$$
$$+ \left(\frac{m}{2} \times H_2O\right) + \left[\left(n + \frac{m}{4}\right) \times 3.76\,N_2\right]. \quad (1)$$

3.1 Energy analysis

First law of thermodynamics expresses the law of conservation and transformation of energy and highlights that energy is a property of thermodynamics. According to the law of conservation and transformation of energy, energy cannot be destroyed or created out of nothing, but it is transformed from one form of energy to another form through various physical and chemical processes. During this transformation, the amount of energy remains constant [42].

In the ICEs, the mass conservation law in a control volume under continuous conditions:

$$\sum \dot{m}_{in} = \sum \dot{m}_{out}. \quad (2)$$

The expression of the energy conservation law:

$$\dot{Q} - \dot{W} = \sum \dot{m}_{out} h_{out} - \sum \dot{m}_{in} h_{in}, \quad (3)$$

where $\dot{m}$, h, $\dot{Q}$, and W refer to the mass flow rate, enthalpy, heat, and power, respectively [44].

In the ICEs, the energy balance takes into account the power and losses acquired from the fuel entering the engine [45]:
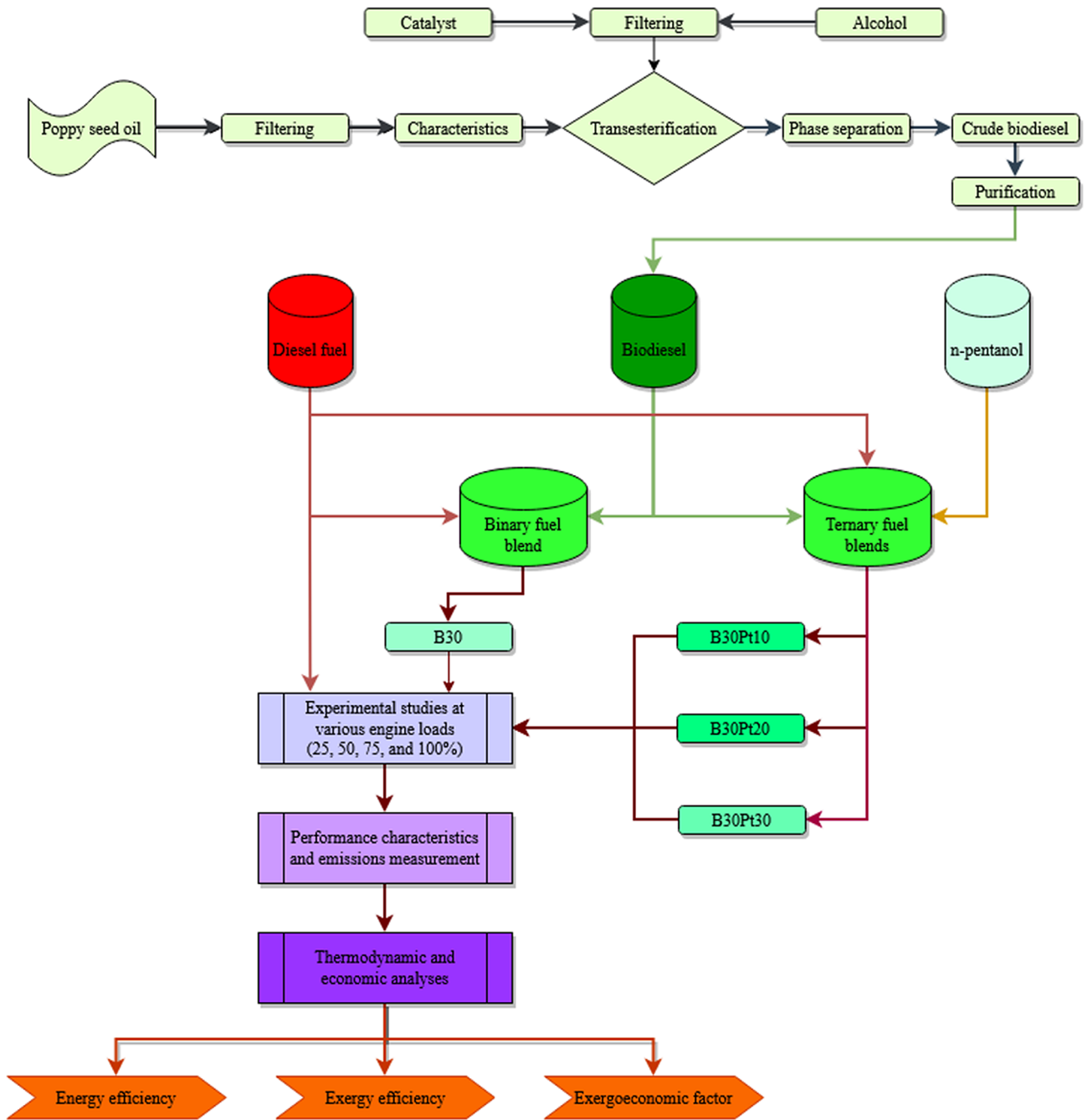
$$\dot{E}_f = \dot{W} + \dot{E}_{ex} + \dot{E}_{cw} + \dot{E}_{loss}. \quad (4)$$

As given in equation (5), $\dot{E}_f$, $\dot{E}_{ex}$, $\dot{E}_{cw}$, and $\dot{E}_{loss}$ point out the energy of the fuel, exhaust energy, cooling water energy, and losses. The energy of the fuel can be determined using the mass flow rate ($\dot{m}_{fuel}$) and lower heating value (H_u) of the fuel. Energy losses refer to the total losses that occur in the engine in different ways such as friction and heat transfer, etc., and are complicated to quantify [46].

$$\dot{E}_f = \dot{m}_f H_u. \quad (5)$$

The losses from the control volume are plotted in Figure 3 [47]:

$$\dot{E}_{loss} = \dot{E}_f - (\dot{W} + \dot{E}_{ex} + \dot{E}_{cw}). \quad (6)$$

Fig. 2. Flowchart of the present study.

The exhaust gas energy [48]:

$$\dot{E}_{ex} = (\dot{m}_f + \dot{m}_{air})c_{ex}(T_{exin} - T_o), \tag{7}$$

where $\dot{m}_{air}$, c_{ex}, T_{exin}, and T_o indicate the air flow rate, exhaust gas specific heat, exhaust gas inlet temperature, and is ambient temperature.

The energy lost by the cooling system of the engine:

$$\dot{E}_{cw} = \dot{m}_{cw}c_{cw}(T_{cw1} - T_{cw2}), \tag{8}$$

where, $\dot{m}_{cw}$, c_{cw}, T_{cw1}, and T_{cw2} are the cooling water flow rate, the specific heat of cooling water, the inlet

temperature of cooling water, and the outlet temperature of cooling water [49].

Thermal efficiency (η) which is the ratio of the power generated in the engine to fuel energy in ICEs [50]:

$$\eta = \frac{\dot{W}}{\dot{E}_f}. \tag{9}$$

3.2 Exergy analysis

Exergy analysis takes place if first and second laws of thermodynamics are satisfied. Exergy is a reversible process.

Fig. 3. Schematic representation of the control volume.

Maximum work is achieved when the environment is in equilibrium with the exergy. We can define exergy as the usable part of the energy and express it as availability [51].

All energy and exergy analysis calculations of the test fuels were calculated by making some assumptions. It is assumed that the engine system is an open system in a steady state and that the inlet air and exhaust gas are ideal gas mixtures. Since the amounts of the kinetic and potential energy of the system are very small compared to the total amount of the system, they are not taken into account in the calculations and their contribution to the system is neglected. In the calculations, the reference ambient temperature and pressure values were taken as $T_0 = 298.15$ K and $P_0 = 100$ kPa, respectively, and were assumed to remain the same throughout the experiment. In addition to the aforesaid assumptions, the reference environment was considered to be an ideal gas [52–55].

In order to understand how efficient the energy conversion is in ICEs, exergy analysis should also be performed in addition to energy analysis. Since exergy analysis is based on the second law of thermodynamics, it generally provides better detection of inefficiencies in the process than energy analysis. In engines, the entrance of the fuel into the engine cylinder, the combustion process, the release of the products from the engine to the external environment after the combustion reaction, friction, and heat transfer result in irreversibilities. These irreversibilities lead to a considerable percentage of the fuel exergy being released outside during power generation. The increase in irreversibilities reduces performance and exergy efficiency. Exergy analysis is

performed to figure out the irreversibilities. The optimum engine operating conditions can be determined with the aforementioned analysis.

In this regard, exergy balance in ICEs [44]:

$$\sum \dot{Ex}_{\mathrm{in}} = \sum \dot{Ex}_{\mathrm{out}} + \dot{Ex}_{\mathrm{dest}}, \qquad (10)$$

where $\dot{Ex}$ demonstrates the exergy flow rate. In addition, the subscripts of in, out, and dest refer to the inlet, outlet, and destruction, respectively. If air enters the control volume under dead-state conditions (usually at atmospheric conditions), $\dot{Ex}_{\mathrm{air}}$ is accepted as zero. However, if the air is admitted under conditions other than dead air, the exergy of the air must be calculated from the following formula:

$$\dot{Ex}_{\mathrm{air}} = \dot{m}_{\mathrm{air}} c_{\mathrm{air}} \left(T_{\mathrm{air}} - T_0 - T_0 \ln \frac{T_{\mathrm{air}}}{T_0} \right) + \dot{m}_{\mathrm{air}} R T_0 \ln \frac{P_{\mathrm{air}}}{P_0},$$
$$(11)$$

where $\dot{m}_{\mathrm{air}}$, c_{air}, T_{air}, and P_{air} show the flow rate of the air, the specific heat of the air, the temperature of the air, and the pressure of the air, respectively.

To conclude, the exergy balance for the test engine:

$$\dot{Ex}_{\mathrm{air}} + \dot{Ex}_{\mathrm{f}} = \dot{Ex}_{\mathrm{work}} + \dot{Ex}_{\mathrm{ex}} + \dot{Ex}_{\mathrm{cw}} + \dot{Ex}_{\mathrm{heat}} + \dot{Ex}_{\mathrm{dest}}, \qquad (12)$$

where $\dot{Ex}$ demonstrates the exergy flow rate. Besides that, the subscripts of air, f, work, ex, cw, and heat point out

Table 3. The mass fractions of the test fuels used in the present analyses.

Fuel	h	o	c	α
B30	0.09952	0.04553	0.85495	0
B30Pt10	0.09125	0.05383	0.85492	0
B30Pt20	0.08275	0.06236	0.85489	0
B30Pt30	0.07402	0.07112	0.85486	0
DF	0.12953	0	0.87047	0

the fuel, work, air, exhaust, cooling water, and heat transfer, respectively. In the meantime, the exergetic net-work is equal to the brake power generated from the test engine ($\dot{E}x_w = \dot{W}$) [56].

In the present analysis, the exergy factor (φ) for liquid fuels:

$$\varphi = 1.0401 + 0.1728\frac{h}{c} + 0.0432\frac{o}{c} + 0.2169\frac{\alpha}{c}\left(1 - 2.0628\frac{h}{c}\right),$$

$$(13)$$

where, h, c, o, and α indicate the proportions of hydrogen, carbon, oxygen, and sulfur in the fuel, respectively. The mass fractions of the test fuels used in the present analyses are shown in Table 3.

The specific exergy (ε_f):

$$\varepsilon_f = H_u\varphi. \quad (14)$$

The exergy of fuel can be calculated with equation (15) using the specific exergy (ε_f) and the lower heating value [57]:

$$\dot{E}x_f = \dot{m}_f\varepsilon_f. \quad (15)$$

The exhaust exergy which is the sum of the physical (ε_{phy}) and chemical (ε_{ch}) exergies of each component (i) [19–22]:

$$\dot{E}x_{ex} = \sum\left(\varepsilon_{phy} + \varepsilon_{ch}\right)_i. \quad (16)$$

Physical exergy [19–22]:

$$\varepsilon_{phy} = \left[(h - T_0 s) - (h_0 - T_0 s_0)\right]. \quad (17)$$

Chemical exergy [19–22]:

$$\varepsilon_{ch} = \overline{R}T_0\ln\frac{1}{y^e}, \quad (18)$$

where s, h, $\overline{R}$, and T show the specific entropy, enthalpy, gas constant, and temperature, respectively. In addition, the index "0" and "e" indicate the dead state and environment, respectively. To calculate the chemical exergy, the amounts of gases used in chemical exergy calculations are assumed to be 75.67%, 20.35%, 0.0345%, 3.03%, and 0.91455% for N_2, O_2, CO_2, H_2O, and other gas components, respectively. [55].

The cooling water exergy [44, 45]:

$$\dot{E}x_{cw} = \sum\left(1 - \frac{T_0}{T_{av}}\right)\dot{Q}_{cw}. \quad (20)$$

The average cooling water temperature (T_{av}):

$$T_{av} = \frac{T_{cwin} + T_{cwout}}{2}, \quad (21)$$

where the subscripts of cwin and cwout refer to the inlet and outlet of the Cooling water, respectively.

Exergy losses occurred during heat transfer [46–48]:

$$\dot{E}x_{heat} = \sum\left(1 - \frac{T_0}{T_s}\right)\dot{Q}_{loss}, \quad (22)$$

where T_s is the engine surface temperature.

Exergy efficiency (ψ) [56, 57]:

$$\psi = \frac{\dot{E}x_w}{\dot{E}x_f}. \quad (23)$$

Exergy destruction [58, 59]:

$$\dot{E}x_{dest} = (\dot{E}x_{air} + \dot{E}x_f) - (\dot{E}x_{work} + \dot{E}x_{ex} + \dot{E}x_{cw} + \dot{E}x_{heat}). \quad (24)$$

Entropy generation ($\dot{S}_{gen}$) [59, 60]:

$$\dot{S}_{gen} = \frac{\dot{E}x_{dest}}{T_0}. \quad (25)$$

3.4 Exergoeconomic analysis

In exergoeconomic analyses, economic and energy-energy analyses are used together to figure out the actual product costs of the systems. In the current analysis, exergy values are considered to be the real data that can be used to determine the interaction of the thermal system with its environment and the cost of thermodynamic inefficiencies within [58]. Fuel flow rate and engine power must be calculated before exergoeconomic analysis is carried out. Moreover, the exergy analysis has to detect the fuel exergy, the exergies of losses, and the exergy lost [57].

The cost balance for the control volume:

$$\dot{C}_f + \dot{C}_a + \dot{Z} = \dot{C}_w + \dot{C}_{exh} + \dot{C}_{loss}, \quad (26)$$

where $\dot{C}$ and $\dot{Z}$ represent the specific cost of exergy and investment cost ratio of the engine, respectively. The subscripts of the present equation are given above. As stated earlier, the exergy cost of air is accepted to be zero.

The specific cost of exergy (c) for each component taking into account the cost per unit of exergy [59]:

$$c_f\dot{E}x_f + \dot{Z} = c_w\dot{E}x_w + c_{exh}\dot{E}x_{exh} + c_{loss}\dot{E}x_{loss}. \quad (27)$$

The fuel taken into the cylinder is consumed to produce power from the engine. In this regard, the cost of the fuel is incurred to acquire power. Therefore, the exergy cost of the exhaust gases and the exergy cost of the heat losses from the engine casing are taken equal per unit of exergy for the fuel, as demonstrated in equation (28) [60]:

$$c_f = c_{exh} = c_{loss}. \quad (28)$$

The final state of the exergoeconomic balance is given in equation (29).

$$c_f \dot{E}x_f + \dot{Z} = c_w \dot{E}x_w + c_f \dot{E}x_{exh} + c_f \dot{E}x_{loss}. \quad (29)$$

The pump prices of DF, PSOB, and n-pentanol in Turkey are approximately 1.1 \$/L, 25.87 \$/L, and 21.17 \$/L, respectively. The unit cost of engine power exergy was calculated from equation (30) [23]:

$$c_w = \frac{c_f \left(\dot{E}x_f - \dot{E}x_{ex} - \dot{E}x_{loss}\right) + \dot{Z}}{\dot{E}x_w}. \quad (30)$$

The investment cost ratio for an ICEs [61]:

$$\dot{Z} = \dot{Z}_{CI} + \dot{Z}_{OM}, \quad (31)$$

where $\dot{Z}_{CI}$ and $\dot{Z}_{OM}$ represent the initial investment cost and the operating cost of the engine, respectively.

The operating cost of the engine as a function of time [62]:

$$\dot{Z}_{OM} = 0.004t + 71.78. \quad (32)$$

In the calculation of $\dot{Z}$, $\dot{Z}_{CI}$ is taken as 6000 \$. It is assumed that the tested engine operates 12 h/day and has an operating life of 20 years. With this data, the total cost rate for the engine is calculated to be 6423 \$ and $\dot{Z}$ is found to be 0.073 \$/h.

The exergoeconomic factor (f) for fuels based on the investment cost ratio and total exergy losses:

$$f = \frac{\dot{Z}}{\dot{Z} + c_f \left(\dot{E}x_{dest} + \dot{E}x_{ex} + \dot{E}x_{loss}\right)}. \quad (33)$$

Relative cost difference (r_c) is calculated from equation (34), as given below.

$$r_c = \frac{c_w - c_f}{c_f}. \quad (34)$$

4 Result and discussion

This study was carried out on a single-cylinder CI engine using different volumetric ratios of DF, PSOB, and n-pentanol fuel blends at a constant speed of 1500 rpm and different loads. The data obtained from these tests are given in Table 4. Energy is released as a result of the combustion of fuels in the cylinder. The combustion of fuels takes place with oxygen supplied from the atmosphere. The combustion of fuel and oxygen in the cylinder releases energy, CO_2, water, and other emissions. These harmful emissions are discharged into the atmosphere through the exhaust.

CI engines can emit emissions such as HC, CO, PM, and NO_X. These emissions harm the environment. Therefore, harmful emissions need to be controlled. In CI engines, emissions can be reduced by intervening in the combustion system or fuel. Fuel intervention is the subject of alternative fuel research. In these studies, the engine system is usually not modified. In order to get full energy from the fuel, the fentire fuel must burn with sufficient oxygen. In CI engines, since the mixture is formed directly in the cylinder, combustion starts before the mixing of air and fuel is completed. This situation causes the presence of unburned gases in the exhaust. Whether the combustion in the engine is complete depends on the amount of air in the combustion chamber where the combustion takes place [63]. If the fuel is not fully combusted as a result of the fuel cycle or if the combustion is interrupted, products such as CO, H_2, and NO are formed in addition to these components. NO_X, CO, HC, SO_X, and soot are the most important pollutant components in CI engines [64].

In this study, energy and exergy analysis was performed using engine performance and emission data. $\dot{m}_f$, $\dot{m}_{air}$, CO emission, CO_2 emission, T_{cw}, and T_{ex} were measured for the five fuel blends and shown in Table 4. Energy and exergy analysis was performed by utilizing these data. In the study, fuel energy, fuel exergy, and thermal losses of fuel blends were calculated. Using equation (5), the energy of the fuel was determined depending on the lower heating value and mass flow rate. The increase in engine load causes an increase in engine torque and power. As can be seen in Table 5, the highest fuel energy at all engine loads and the highest fuel consumption is B30Pt30 fuel. Since the difference between the lower heating values of the fuel blends is not very high, fuel consumption is an important parameter determining the fuel energy. The lowest fuel energy at all engine loads is for DF. For DF, it is 7.052, 8.289, 12.141, and 15.014 kW for 25, 50, 75, and 100% engine loads, respectively. In the triple fuel blends, the PSOB ratio is taken fixed at 30%. In these fuel blends, the increase in n-pentanol content promotes fuel consumption and consequently fuel energy. At 100% load, the fuel energy of B30Pt10, B30Pt20, and B30Pt30 fuels are 17.852, 18.346, and 20.010 kW, respectively. Under the same conditions, the inlet energy of B30 fuel is 16.846 kW. The increase in engine load increases the fuel energy.

Thermal losses in the control volume depend on the energy of the fuel, engine power, energy of exhaust gases, and heat transferred to the cooling water. When Table 5 is examined, it is seen that thermal losses increase as the engine load increases in fuel blends. At 100% engine load of B30 fuel, the heat transferred to the cooling water and exhaust energy is 2.401 and 2.438 kW, respectively. Under the same conditions, B30Pt30 fuel is calculated as 2.731 and 2.752 kW. The addition of n-pentanol in fuel blends increases fuel consumption and causes an increase in the combustion temperature in the cylinder. In the study, the exergy of fuel blends was calculated. Calculations in fuel exergy are similar to fuel energy. The exergy of fuel is higher than the fuel energy because the chemical exergy factor is greater than 1. Although the lower heating value of B30 fuel is lower than that of DF, the specific fuel consumption exergy is also higher because the fuel consumption is higher.
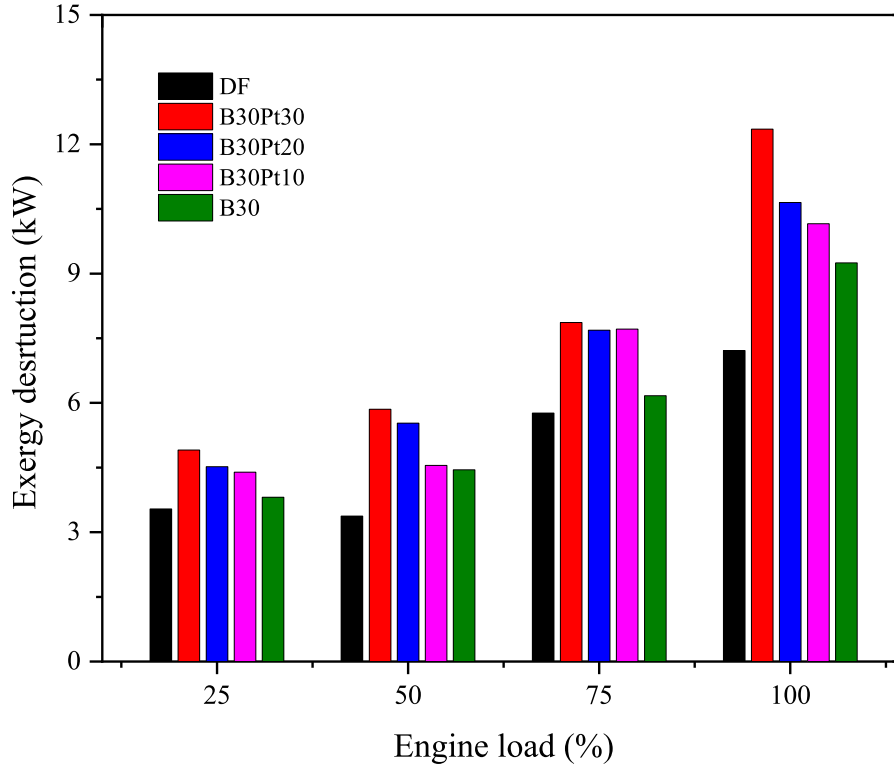
The exergy of cooling water varies depending on the temperature. Higher cooling water exergy is calculated for the DF-PSOB binary fuel blend compared to DF. The addition of n-pentanol to this binary fuel blend causes an increase in the cooling water exergy. The combustion temperature in the cylinder increases due to the oxygen content of alcohol. However, the lower energy content of n-pentanol resulted in the engine consuming more fuel to deliver the same power output. This increases the combustion chamber

Table 4. Performance and emission data used in thermodynamic analysis.

Fuel	Load (%)	$\dot{m}_f$ (kg/h)	$\dot{m}_{air}$ (kg/h)	CO (%)	CO_2 (%)	T_{cw} (°C)	T_{ex} (°C)
DF	25	0.574	31.091	0.12	4.47	46.50	185
	50	0.675	30.133	0.16	6.40	48.50	260
	75	0.989	29.398	0.44	8.58	49.80	340
	100	1.223	28.691	1.33	10.98	49.82	386
B30Pt30	25	0.744	31.159	0.22	4.31	50.88	196
	50	0.951	29.691	0.18	6.40	55.06	271
	75	1.259	29.216	0.22	8.68	58.56	350
	100	1.779	28.542	0.58	11.08	62.74	401
B30Pt20	25	0.700	31.044	0.22	6.01	47.70	203
	50	0.912	29.922	0.16	5.98	51.33	282
	75	1.224	29.102	0.16	6.01	57.25	362
	100	1.598	28.542	0.55	11.07	57.38	412
B30Pt10	25	0.680	30.562	0.16	6.01	48.02	216
	50	0.802	29.874	0.15	8.43	50.77	293
	75	1.181	29.163	0.16	11.12	53.31	371
	100	1.524	28.253	0.62	13.64	56.45	421
B30	25	0.611	30.789	0.14	4.43	43.89	231
	50	0.776	29.991	0.12	6.50	46.87	332
	75	1.039	29.378	0.21	8.64	50.42	385
	100	1.410	28.404	0.99	11.21	53.51	440

Table 5. The outcomes obtained from thermodynamic analysis in the present study.

Fuel	Load (%)	Fuel energy (kW)	Exhaust energy (kW)	Coolant energy (kW)	Fuel exergy (kW)	Coolant exergy (kW)	Exhaust exergy (kW)
DF	25	7.052	1.393	1.423	7.552	0.170	2.544
	50	8.289	1.672	1.723	8.877	0.173	2.729
	75	12.141	1.916	1.967	13.001	0.360	2.958
	100	15.014	2.951	2.080	16.078	0.488	3.174
B30Pt30	25	8.367	1.393	1.579	8.985	0.262	2.515
	50	10.700	1.533	1.962	11.490	0.338	2.699
	75	14.163	1.916	2.309	15.208	0.498	2.924
	100	20.010	2.752	2.731	21.487	0.832	3.103
B30Pt20	25	8.036	1.533	1.584	8.617	0.234	2.562
	50	10.466	1.533	1.965	11.223	0.322	2.770
	75	14.052	1.916	2.253	15.068	0.481	2.980
	100	18.346	2.717	2.290	19.673	0.719	3.105
B30Pt10	25	7.965	1.393	1.555	8.529	0.232	2.605
	50	9.396	1.707	1.920	10.061	0.250	2.662
	75	13.834	2.055	2.273	14.813	0.481	2.698
	100	17.852	2.752	2.657	19.116	0.684	3.076
B30	25	7.303	1.428	1.196	7.808	0.188	2.507
	50	9.269	0.941	1.581	9.911	0.244	2.619
	75	12.408	1.986	2.021	13.267	0.381	2.797
	100	16.846	2.438	2.401	18.012	0.617	2.946

Fig. 4. Variation of exergy destruction depending on the ranging engine loads.
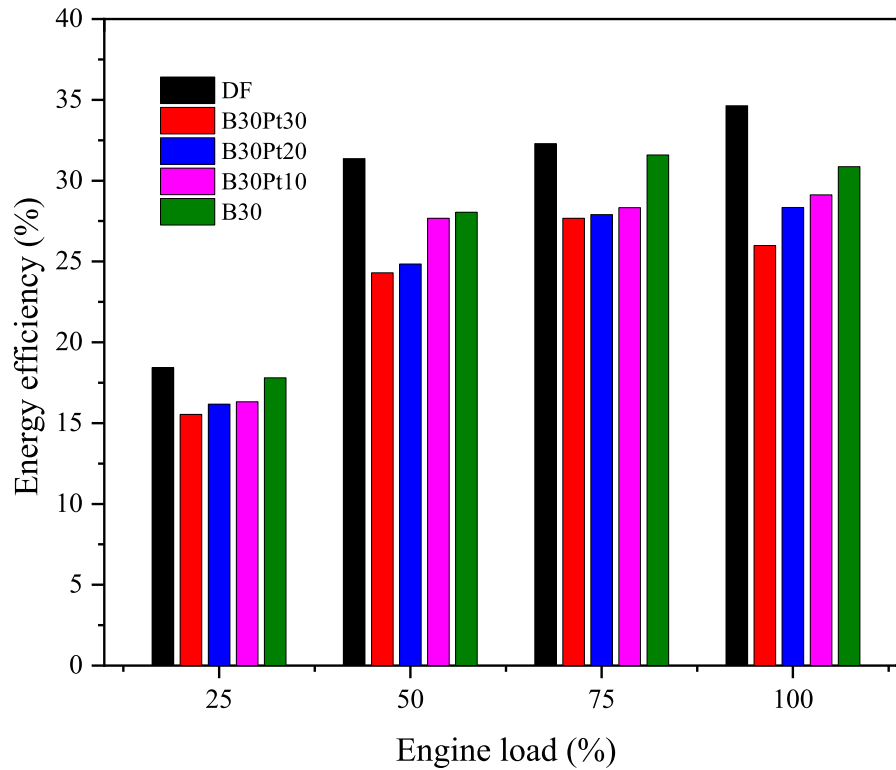
temperature and increases the amount of heat transferred to the engine coolant. This increases the energy and exergy of the water sent for cooling. In Table 4, cooling water temperatures were determined as 49.82, 62.74, 57.30, 56.45, and 53.51 °C for DF, B30Pt30, B30Pt20, B30Pt10, and B30 fuels, respectively at the highest load. Cooling water temperatures were calculated as 48.50, 55.06, 51.33, 50.77, and 46.87 °C for DF, B30Pt30, B30Pt20, B30Pt10, and B30 fuels, respectively at 50% load. As can be seen, cooling water temperatures increase as the alcohol content increases. In Table 5, the cooling water exergy is calculated as 0.488, 0.832, 0.719, 0.684, and 0.617 kW for DF, B30Pt30, B30Pt20, B30Pt10, B30Pt10, and B30 fuels at the maximum load and corresponds 0.173, 0.338, 0.322, 0.250, and 0.244 kW at 50% load, respectively. At all engine loads, the augmentation in cooling water temperature increased the cooling water exergy.

Exhaust exergy increases with increasing engine load. The increase in engine load leads to an increase in fuel consumption. This increases the amount and temperature of exhaust gases. As the temperature of the exhaust gases increases, it is inevitable that the exhaust exergy increases. When the exhaust gas temperature is examined in Table 4; at 100, 75, 50, and 25% engine loads, the exhaust gas temperature values for DF were measured as 386, 340, 260, and 185 °C, respectively. At 100, 75, 50, and 25%, the exhaust gas temperature for B30Pt30 fuel was recorded to be 196, 271, 350, and 401 °C, respectively. The exhaust gas exergy in Table 5 shows that the exhaust gas exergy values for DF were found to be 3.174 kW for 100% load,

2.958 kW for 75% load, 2.729 kW for 50% load, and 2.544 kW for 25% load. For B30Pt30 fuel, it was calculated as 3.103 kW for 100% load, 2.924 kW for 75% load, 2.699 kW for 50% load, and 2.515 kW for 25% load, respectively. As observed, in the case of increasing the engine load, the exhaust gas temperature also increases. The increase in exhaust gas temperature increases the exhaust gas exergy.

According to the first law of thermodynamics, energy is conserved but there is no conservation of exergy. The difference between the exergy in and exergy out in a system is exergy dissipation. Exergy dissipation occurs in all real systems. In the ICEs, the exergy of fuel and air is used to generate power in the engine. The resulting exhaust and cooling water losses will have exergy dissipation, which refers to the exergy of the exhaust and cooling water losses, as well as other unaccounted-for and undetermined losses. Figure 4 shows the exergy destruction values of the fuel blends. Exergy destruction is highest at 100% engine load for all fuel blends. It is calculated as 7.216, 12.353, 10.650, 10.153, and 9.249 kW at 100% load for DF, B30Pt30, B30Pt20, B30Pt10, and B30 fuels, respectively.

Figure 5 shows the thermal efficiency results at different engine speeds. Thermal efficiency values generally decrease with increasing engine load. As the engine load ascends, the friction losses increase, resulting in a reduction in thermal efficiency. However, increasing engine speed can also increase the amount of power generated by the engine, so the overall efficiency of the engine can change. The test fuels were analyzed at four different engine loads (25, 50, 75, 100%). The highest thermal efficiency was observed for DF.

Fig. 5. Variation of thermal efficiency depending on the ranging engine loads.

At 25% engine load, the thermal power of DF was 18.43 kW, while the thermal power of DF at full load was 34.63 kW. For B30Pt30 fuel, it was calculated as 15.54 kW at 25% engine load and 25.99 kW at 100% engine load. For all test fuels, increasing the engine load increased the thermal efficiency.

Figure 6 displays the exergy efficiency graph at different engine loads. Engine loads are taken as (25–100%). Among the fuels, DF has the highest exergy efficiency at all engine loads. For DF, it was calculated as 32.34 kW at 100% engine load, 32.29 kW at 75% engine load, 31.37 kW at 50% engine load, and 17.21 kW at 25% engine load. B30Pt30 fuel was found to have the lowest exergy efficiency. The exergy values of B30Pt30 fuel were 24.20 kW for 100% engine load, 27.68 kW for 75% engine load, 24.30 kW for 50% engine load, and 14.47 kW for 25% engine load. As the engine load increased, the exergy values of all test fuels increased.

Figure 7 presents the fuel cost ratios of the test fuels at different engine loads. The increase in engine load leads to an increase in fuel consumption, which in turn increases the fuel-cost ratio. Attributable to the high pump prices of PSOB and n-pentanol, the cost ratio is significantly higher for dual and triple fuel blends than for DF. In B30, B30Pt10, B30Pt20, and B30Pt30 fuel blends, the commercial DF volumetric ratio is 70%, 60%, 50%, and 40% respectively. Therefore, the fuel cost rate of these fuels is affected by commercial DF, which has an extremely low pump price compared to PSOB and n-pentanol. DF has the lowest cost rate due to its low pump price and the lowest fuel consumption in engine tests. At 100% engine load, the fuel cost rates of DF, B30, and B30Pt30 fuels are found to be 1.63, 15.52, and 30.71 \$/h, respectively. In PSOB-DF binary fuel blends, the fuel cost ratio increases with an increasing n-pentanol ratio. When the engine load is 75%, the fuel cost rates are 14.72, 18.20, and 21.74 \$/h for B30Pt10, B30Pt20, and B30Pt30 fuels, respectively.

The cost of power (c_w) from the crankshaft is an important parameter for the assessment of fuel blends in alternative fuel research. The goal of the exergoeconomic analysis is to determine the c_w taken from the crankshaft and losses. In the study, c_w taken from the crankshaft was calculated and given in Figure 8. The increase in engine load reduced c_w taken from the crankshaft. For example, for B30Pt30 fuel at 25, 50, 75, and 100% loads, c_w figures were found to be 8826, 5712, 5671, and 5297 \$/GJ, respectively. For B30 fuel and DF, c_w at 100% engine load is calculated as 2126.77 and 211.86 \$/GJ, respectively. The lower pump price of DF reduces the power cost of DF. With the addition of n-pentanol to B30 fuel, c_w increases. At 50% engine load, c_w values for B30Pt10, B30Pt20, and B30Pt30 fuels are 3120.5, 4535.36, and 5712 \$/GJ respectively. The reason why B30Pt30 fuel has a very high cost compared to the others is the low proportion of commercial DF in the fuel mix.

In the economic analysis of ICEs, evaluations based on the initial investment cost lead to misguidance. Operating and maintenance costs throughout the life of an engine are more important than the initial investment cost. The exergoeconomic factor (f) calculated in exergoeconomic analysis shows the relationship between initial investment cost and operation and maintenance costs. In this study,
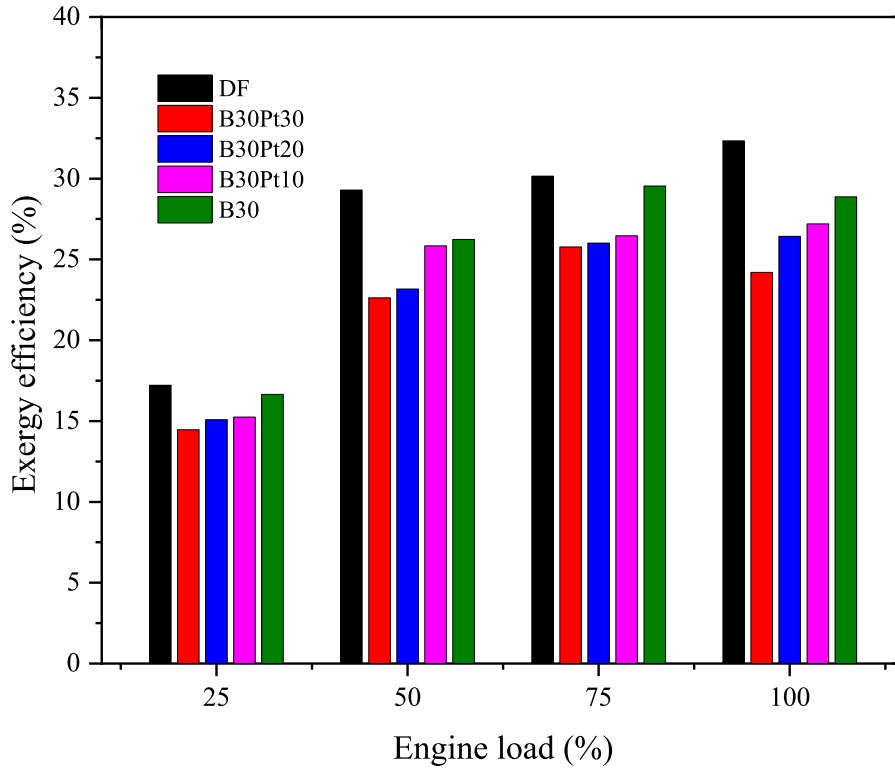
Fig. 6. Variation of exergy efficiency depending on the ranging engine loads.
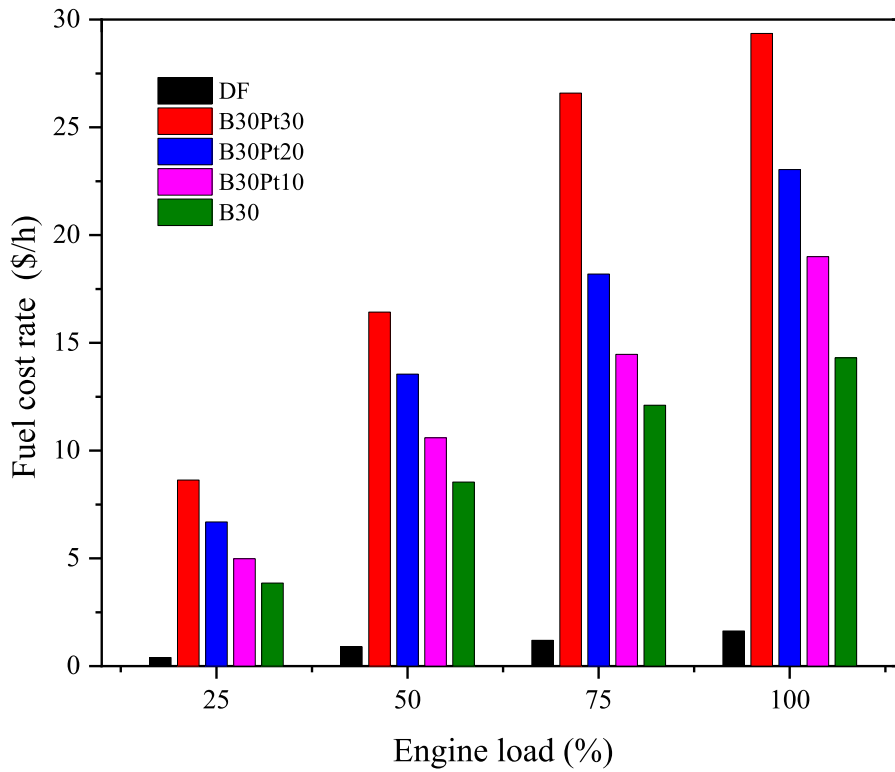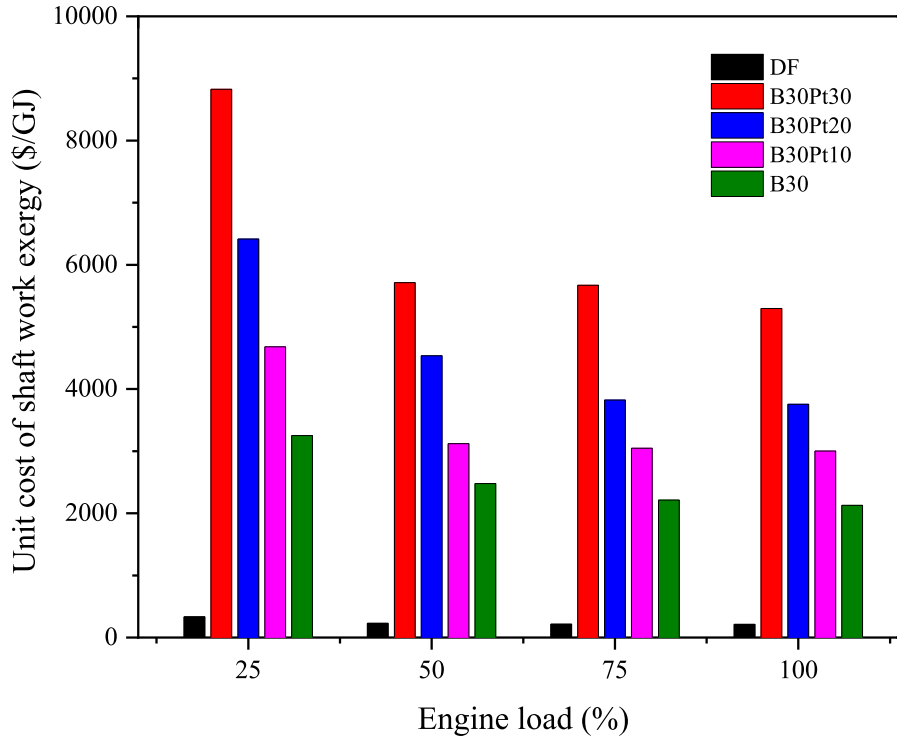

Fig. 7. Variation of fuel cost rate depending on the ranging engine loads.

Fig. 8. Variation of unit cost of shaft work exergy depending on the ranging engine loads.

different fuels were tested without any modifications to the engine. Therefore, the initial investment cost of the engine is taken constant for all fuel blends. Therefore, the change in f depends on the cost of exergy losses. In this case, f depends on the exergy losses. If two fuels with the same exergy losses are considered, the cost of exergy losses of the fuel with higher pump prices will be higher. Since the cost of exergy losses is in the denominator in equation (33), f will decline as the cost of these losses increases. f values of all fuels in the study are given in Figure 9. At 100% engine load, f of DF is about 11 times higher than B30 fuel. This is assignable to fuel pump prices. The addition of n-pentanol to B30 fuel results f to decline. f of B30 Pt10 fuel at 100% engine load is about 2 times that of B30Pt30 fuel. Cavalcanti *et al.* [27], in their study, calculated f between 0.3555% (D95B5) and 0.1613% (B100) for 9 kW. As the biodiesel concentration increases, the amount of oxygen in the DF structure and the combustion characteristics of the fuel change, which may have an impact on engine performance and exhaust emissions. Therefore, they found the lowest f values of pure biodiesel (0.1613, 0.1322, and 0.1107% for 9, 18, and 27 kW respectively). The researchers noted that these results show the worst performance in exergoeconomic terms. Açıkkalp *et al.* [65] made calculations according to traditional exergoeconomic analysis. f is a concept that evaluates the energy efficiency and economic performance of a system together. The researchers encountered the maximum f to be 0.355. Aghbashlo *et al.* [28] found f to be as low as 4.27% for B5W5m at 100% load and 23.60% for B5W3m fuel at 25% engine load. Yildirim and Gungor [66] calculated f of a CI engine as 79.86%.

Figure 10 demonstrates the variation of relative cost difference (r_c) for tested fuel blend types depending on the ranging engine loads. r_c would increase as the unit cost of the engine's exergetic power increases. It will decrease when the losses increase to the exergy cost. A higher r_c means that the fuel will be used at less cost. Therefore, the lowest r_c value is calculated for DF at all engine loads. r_c descends as the engine loads increase. As n-pentanol is added to B30 fuel, r_c increases as the proportion of commercial DF in the mixture decreases. At 100% engine load, r_c for B30Pt10 and B30Pt30 fuels are 1.957 and 2.378, respectively. When the engine load is 25% for the same fuels, r_c is calculated as 3.393 and 3.784, respectively. Aghbashlo *et al.* [1], for example, reported that the efficient use of fuel increases as the engine load increases, resulting in smaller r_c at higher loads. In order to understand how different fuel blends and engine conditions affect work exergy unit costs, they reported that motor vehicles, power plants, and other motorized systems can help in determining the most economical option when making fuel selection. They also calculated that the relative cost differences of fuel blends applied for dissimilar loads and speeds ranged from 0.87 to 4.22. Cavalcanti *et al.* [27] indicated that r_c decreased as the load rose. For 9 kW, it could be concluded that r_c varies between 3.18 and 3.128 for different fuels. On the other hand, r_c value ranged between 1.396 and 1.44 for 27 kW.

The c_w generated from an ICE is much higher than the initial investment cost. Therefore, the sustainability of the fuel employed is important for engine operation. As known, sustainable development is a strategy that consolidates economic progress, social comfort, and environmental concern. In this sense, the augmentation in the energy
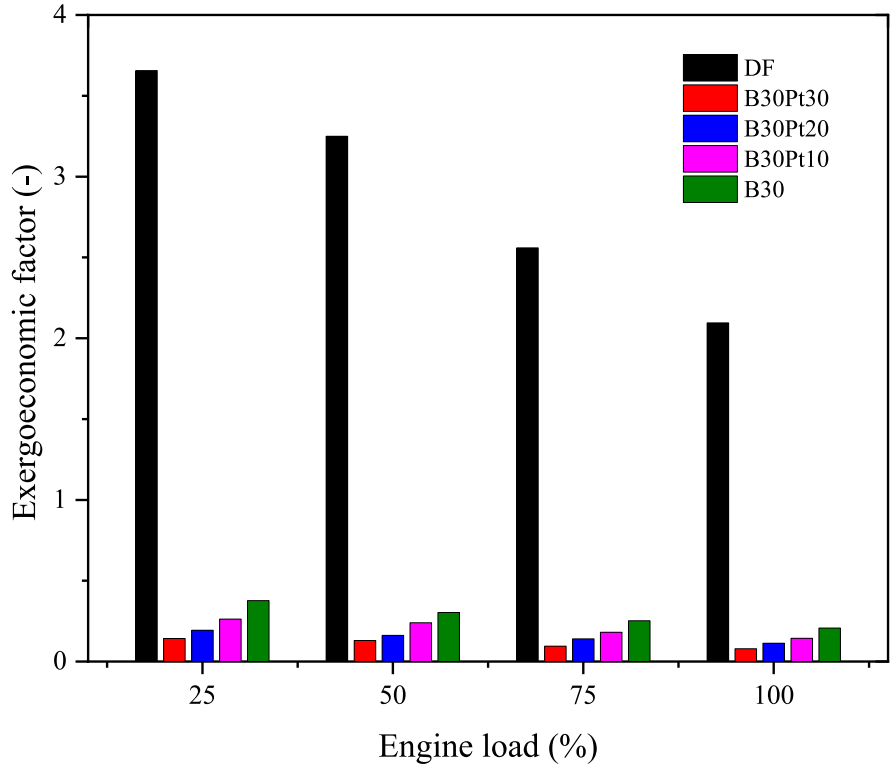
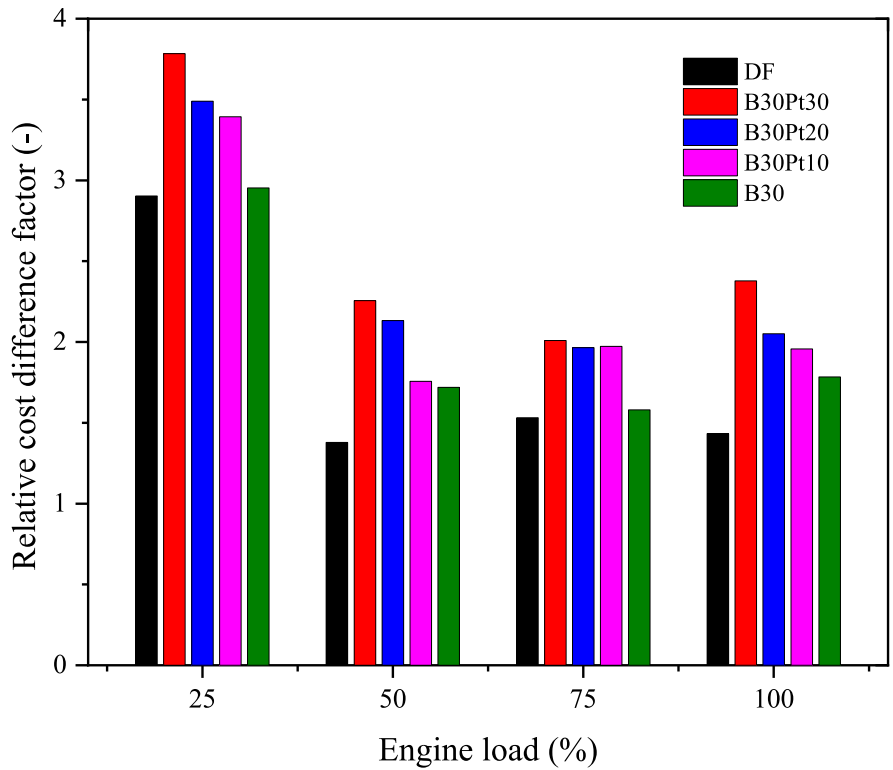**Fig. 9.** Variation of exergoeconomic factors depending on the ranging engine loads.

Fig. 10. Variation of relative cost difference factor depending on the ranging engine loads.
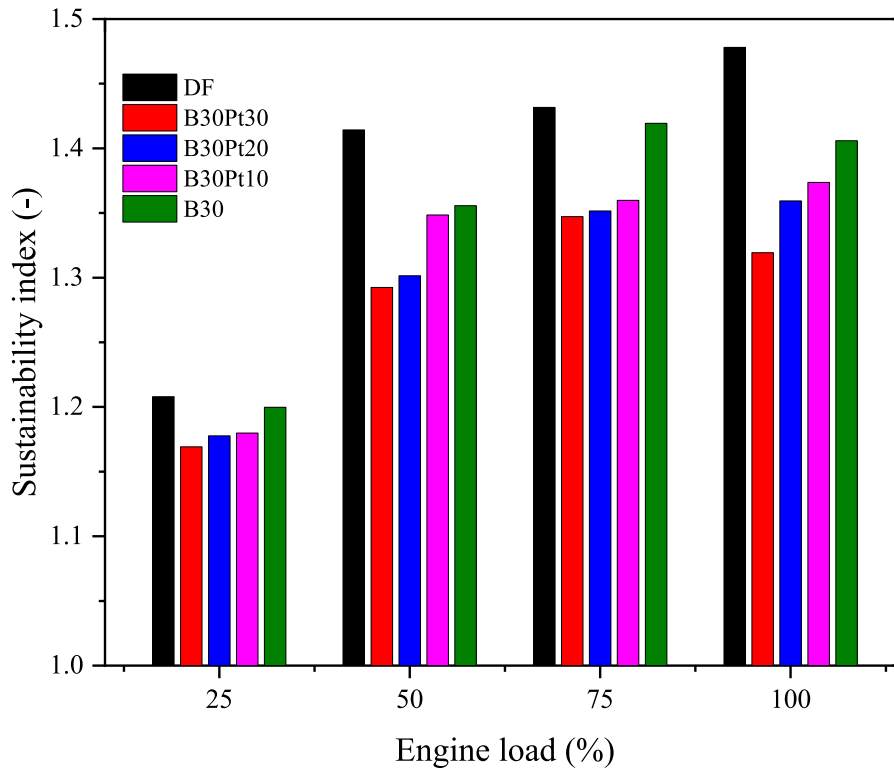
Fig. 11. Variation of sustainability index depending on the ranging engine loads.

Table 6. Comparison of findings coming from the present study (lowest to highest).

Parameter	Order
Energy efficiency	B30Pt30 < B30Pt20 < B30Pt10 < B30 < DF
Exergy efficiency	B30Pt30 < B30Pt20 < B30Pt10 < B30 < DF
Exergy destruction	DF < B30 < B30Pt10< B30Pt20 < B30Pt30
Fuel cost rate	DF < B30 < B30Pt10< B30Pt20 < B30Pt30
Unit cost of shaft work exergy	DF < B30 < B30Pt10< B30Pt20 < B30Pt30
Exergoeconomic factor	B30Pt30 < B30Pt20 < B30Pt10 < B30 < DF
Relative cost difference factor	DF < B30 < B30Pt10< B30Pt20 < B30Pt30
Sustainability index	B30Pt30 < B30Pt20 < B30Pt10 < B30 < DF

requisition in the world will result in hard on account of arriving at the targets. Therefore, it has evolved into an obligation for countries in order to encourage sustainable development. This fact is that ascending energy and exergy efficiency, supporting the utilization of sustainable energy sources, practically declines the influence of energy requests all over the world. SI is a significant parameter in order to compare various fuels used in the engine. If this index is greater than 1, the use of the fuel is considered appropriate. In the study, as shown in Figure 11, SI ascends as the increase in engine load positively affects the exergetic efficiency. SI of DF is higher than that of B30 fuel. At the highest load, SI figures of DF and B30 fuels were calculated to be 1.478 and 1.406, respectively. SI reduces with the infusion of n-pentanol to B30 fuel. At 100% load, the SI of B30Pt10 and B30Pt30 fuel blends are 1.374 and 1.319, respectively. A compatible outcome was presented by Uysal *et al.* [67] who calculated that D85B15 fuel has the highest improvement potential values at all engine loads. They also noted that D85B15GO100 has the lowest improvement potential at every engine load except 6 Nm. This case indicates that D85B15GO100 was the most efficient fuel. The researchers observed at the load of 3 Nm the improvement potential as 3.4928 kW for DF, 3.6396 kW for D85B 3.5477 kW for D85B15GO500, 3.4111 kW for D85B15GO100, and 3.6080 kW for D85B15GO1000. The researchers notified the SI value for D85B15 fuel to be 1.144, 1.245, 1.323, and 1.348 under the load of 3 6, 9, and 12 Nm, respectively.

5 Comparison of present findings with latest literature

Table 6 tabulates the comparison of findings coming from the experimental study (lowest to highest) at the following operating conditions: varying engine loads (from 25% to full load) and constant speed (1500 rpm). It is to be noted that all thermodynamic and economic parameters have been comprehensively compared for each fuel. All the parameters have been demonstrated in ascended order for better evaluation. As observed, DF is the best fuel in terms of energetic and exergetic performance in the CI engine. On the other hand, the price of n-pentanol and poppy seed oil can result in a decrease in the fuel cost rate. In this sense, more sustainable fuel combinations can be obtained shortly. Besides that, attaching several renewable energy technologies to the biodiesel production units has to be taken into consideration as a remarkable research direction so as to increase the sustainability and renewability of the aforementioned systems.

6 Conclusions

Due to constantly decreasing fossil sources, rising energy prices, and environmental issues, the attention to alternative energy resources increases day by day in the world. This extension has come to the fore, especially for vegetable oils with a high scope of services. Being an agricultural country, it has great potential to exhibit force under the gasoline chamber, which makes it possible to make the device possible of vegetable oils as fuel. For the use of fuel in transportation and industrial applications, economics is as important as performance and emissions. Today, the costs of alcohol and PSOB production are higher than the costs of fossil fuels. Therefore, the cost is seen as the biggest obstacle to the usage of alternative fuels in CI engines. In the present examination, five different fuel blends prepared using DF, PSOB, and alcohol were tested in a CI engine at a stable speed (1500 rpm) and different engine loads. Energy, exergy, and exergoeconomic analyses were conducted using the test data. In this context, the highest exergy efficiency for binary and ternary fuel blends is 28.87% for B30 fuel at the maximum load. At the same engine load, it is 24.20% for B30Pt30 fuel. Compared to commercial DF, the exergetic efficiency of B30 and B30Pt30 test fuels were found to be 10.73% and 25.73% lower, respectively at the same engine load. When c_w taken from the crankshaft was analyzed, the cost of B30 and B30Pt30 fuels was observed to be very high compared to DF at all engine loads. While there are not very high differences in the exergy efficiency of commercial DF with binary and ternary blends, this difference in c_w from the crankshaft can be eliminated by reducing the cost of PSOB and alcohol production.

Data availability

Data used in this paper will be supplied at a reasonable request.

References

1 Aghbashlo M., Tabatabaei M., Mohammadi P., Khoshnevisan B., Rajaeifar M.A., Pakzad M. (2017) Neat diesel beats waste-oriented biodiesel from the exergoeconomic and exergoenvironmental point of views, *Energy Convers. Manag.* **148**, 1–15. https://doi.org/10.1016/j.enconman.2017.05.048.

2 Odibi C., Babaie M., Zare A., Nabi M.N., Bodisco T.A., Brown R.J. (2019) Exergy analysis of a diesel engine with waste cooking biodiesel and triacetin, *Energy Convers. Manag.* **198**, 111912. https://doi.org/10.1016/j.enconman.2019.111912.

3 Dhanasekaran R., Krishnamoorthy V., Rana D., Saravanan S., Nagendran A., Kumar B.R. (2017) A sustainable and eco-friendly fueling approach for direct-injection diesel engines using restaurant yellow grease and n-pentanol in blends with diesel fuel, *Fuel* **193**, 419–431. https://doi.org/10.1016/j.fuel.2016.12.030.

4 Çakmak A., Yeşilyurt M.K., Erol D., Doğan B. (2022) The experimental investigation on the impact of n-octanol in the compression-ignition engine operating with biodiesel/diesel fuel blends: exergy, exergoeconomic, environmental analyses, *J. Therm. Anal. Calorim.* **147**, 20, 11231–11259. https://doi.org/10.1007/s10973-022-11357-w.

5 Balki M.K., Sayin C., Canakci M. (2014) The effect of different alcohol fuels on the performance, emission and combustion characteristics of a gasoline engine, *Fuel* **115**, 901–906. https://doi.org/10.1016/j.fuel.2012.09.020.

6 Kadian A.K., Khan M., Sharma R.P. (2022) Performance enhancement and emissions mitigation of DI-CI engine fuelled with ternary blends of jatropha biodiesel-diesel-heptanol, *Mater. Sci. Energy Technol.* **5**, 145–154. https://doi.org/10.1016/j.mset.2022.01.002.

7 Zapata-Mina J., Restrepo A., Romero C., Quintero H. (2020) Exergy analysis of a diesel engine converted to spark ignition operating with diesel, ethanol, and gasoline/ethanol blends, *Sustain. Energy Technol. Assess.* **42**, 100803. https://doi.org/10.1016/j.seta.2020.100803.

8 Bhurat S.S., Pasupuleti S.R., Kunwer R., Gugulothu S.K., Joshi S.K. (2022) Effect of ethanol-diesel blend on compression ignition engine: A mini review, *Mater. Today Proc.* **69**, 2, 459–462. https://doi.org/10.1016/j.matpr.2022.09.139.

9 Zhen X., Wang Y. (2015) An overview of methanol as an internal combustion engine fuel, *Renew. Sust. Energy Rev.* **52**, 477–493. https://doi.org/10.1016/j.rser.2015.07.083.

10 Yilmaz N., Atmanli A. (2017) Experimental assessment of a diesel engine fueled with diesel-biodiesel-1-pentanol blends, *Fuel* **191**, 190–197. https://doi.org/10.1016/j.fuel.2016.11.065.

11 Yesilyurt M.K. (2020) A detailed investigation on the performance, combustion, and exhaust emission characteristics of a diesel engine running on the blend of diesel fuel, biodiesel and 1-heptanol (C7 alcohol) as a next-generation higher alcohol, *Fuel* **275**, 117893. https://doi.org/10.1016/j.fuel.2020.117893.

12 Manesh M.K., Navid P., Baghestani M., Abadi S.K., Rosen M.A., Blanco A.M., Amidpour M. (2014) Exergoeconomic and exergoenvironmental evaluation of the coupling of a gas fired steam power plant with a total site utility system,

Energy Convers. Manag. **77**, 469–483. https://doi.org/10.1016/j.enconman.2013.09.053.

13 Ding P., Yuan Z., Shen H., Qi H., Yuan Y., Wang X., Sobhani B. (2020) Exergoeconomic analysis and optimization of a hybrid Kalina and humidification-dehumidification system for waste heat recovery of low-temperature Diesel engine, *Desalination* **496**, 114725. https://doi.org/10.1016/j.desal.2020.114725.

14 Shelar M., Kulkarni G.N. (2016) Thermodynamic and economic analysis of diesel engine based trigeneration systems for an Indian hotel, *Sustain. Energy Technol. Assess.* **13**, 60–67. https://doi.org/10.1016/j.seta.2015.11.008.

15 Mao Y., Zhang L., Wan L., Stanford R.J. (2022) Proposal and assessment of a novel power and freshwater production system for the heat recovery of diesel engine, *Energy* **240**, 122615. https://doi.org/10.1016/j.energy.2021.122615.

16 Çetin O., Sogut M.Z. (2021) A new strategic approach of energy management onboard ships supported by exergy and economic criteria: A case study of a cargo ship, *Ocean Eng.* **219**, 108137. https://doi.org/10.1016/j.oceaneng.2020.108137.

17 Cavalcanti E.J. (2021) Energy, exergy and exergoenvironmental analyses on gas-diesel fuel marine engine used for trigeneration system, *Appl. Therm. Eng.* **184**, 116211. https://doi.org/10.1016/j.applthermaleng.2020.116211.

18 Krishnamoorthi M., Sreedhara S., Duvvuri P.P. (2020) Experimental, numerical and exergy analyses of a dual fuel combustion engine fuelled with syngas and biodiesel/diesel blends, *Appl. Energy* **263**, 114643. https://doi.org/10.1016/j.apenergy.2020.114643.

19 Hosseinzadeh-Bandbafha H., Rafiee S., Mohammadi P., Ghobadian B., Lam S.S., Tabatabaei M., Aghbashlo M. (2021) Exergetic, economic, and environmental life cycle assessment analyses of a heavy-duty tractor diesel engine fueled with diesel–biodiesel-bioethanol blends, *Energy Convers. Manag.* **241**, 114300. https://doi.org/10.1016/j.enconman.2021.114300.

20 Zhu S., Ma Z., Zhang K., Deng K. (2020) Energy and exergy analysis of a novel steam injected turbocompounding system applied on the marine two-stroke diesel engine, *Energy Convers. Manag.* **221**, 113207. https://doi.org/10.1016/j.enconman.2020.113207.

21 Vandani A.M.K., Joda F., Boozarjomehry R.B. (2016) Exergic, economic and environmental impacts of natural gas and diesel in operation of combined cycle power plants, *Energy Convers. Manag.* **109**, 103–112. https://doi.org/10.1016/j.enconman.2015.11.048.

22 Nabi M.N., Rasul M.G., Arefin M.A., Akram M.W., Islam M.T., Chowdhury M.W. (2021) Investigation of major factors that cause diesel NOx formation and assessment of energy and exergy parameters using e-diesel blends, *Fuel* **292**, 120298. https://doi.org/10.1016/j.fuel.2021.120298.

23 Khoobbakht G., Akram A., Karimi M., Najafi G. (2016) Exergy and energy analysis of combustion of blended levels of biodiesel, ethanol and diesel fuel in a DI diesel engine, *Appl. Therm. Eng.* **99**, 720–729. https://doi.org/10.1016/j.applthermaleng.2016.01.022.

24 Paul A., Panua R., Debroy D. (2017) An experimental study of combustion, performance, exergy and emission characteristics of a CI engine fueled by Diesel-ethanol-biodiesel blends, *Energy* **141**, 839–852. https://doi.org/10.1016/j.energy.2017.09.137.

25 da Costa Y.J.R., de Lima A.G.B., Bezerra Filho C.R., de Araujo Lima L. (2012) Energetic and exergetic analyses of a dual-fuel diesel engine, *Renew. Sust. Energy Rev.* **16**, 7, 4651–4660. https://doi.org/10.1016/j.rser.2012.04.013.

26 Taghavifar H., Nemati A., Walther J.H. (2019) Combustion and exergy analysis of multi-component diesel-DME-methanol blends in HCCI engine, *Energy* **187**, 115951. https://doi.org/10.1016/j.energy.2019.115951.

27 Cavalcanti E.J., Carvalho M., Ochoa A.A. (2019) Exergoeconomic and exergoenvironmental comparison of diesel-biodiesel blends in a direct injection engine at variable loads, *Energy Convers. Manag.* **183**, 450–461. https://doi.org/10.1016/j.enconman.2018.12.113.

28 Aghbashlo M., Tabatabaei M., Khalife E., Shojaei T.R., Dadak A. (2018) Exergoeconomic analysis of a DI diesel engine fueled with diesel/biodiesel (B5) emulsions containing aqueous nano cerium oxide, *Energy* **149**, 967–978. https://doi.org/10.1016/j.energy.2018.02.082.

29 Suresh S., Sinha D., Murugavelh S. (2016) Biodiesel production from waste cotton seed oil: Engine performance and emission characteristics, *Biofuels* **7**, 6, 689–698. https://doi.org/10.1080/17597269.2016.1192442.

30 Atabani A.E., Mahlia T.M.I., Masjuki H.H., Badruddin I.A., Yussof H.W., Chong W.T., Lee K.T. (2013) A comparative evaluation of physical and chemical properties of biodiesel synthesized from edible and non-edible oils and study on the effect of biodiesel blending, *Energy* **58**, 296–304. https://doi.org/10.1016/j.energy.2013.05.040.

31 Atabani A.E., Silitonga A.S., Badruddin I.A., Mahlia T.M.I., Masjuki H., Mekhilef S. (2012) A comprehensive review on biodiesel as an alternative energy resource and its characteristics, *Renew. Sust. Energy Rev.* **16**, 4, 2070–2093. https://doi.org/10.1016/j.rser.2012.01.003.

32 Çengelci E., Bayrakçeken H., Aksoy F. (2011) Hayvansal ve bitkisel yağlardan elde edilen biyodizelin dizel yakıtı ile karşılaştırılması, *Electr. J. Veh. Technol.* **3**, 1, 41–53. (in Turkish)

33 Eliçin A.K., Gezici M., Erdoğan D. (2011) Determination of using possibilities of some oil esters as a fuel in a small internal combustion engine, in: 11th International Congress on Mechanization and Energy in Agriculture, Istanbul, Turkey, 21–23 September, pp. 608–613.

34 Imdadul H.K., Masjuki H.H., Kalam M.A., Zulkifli N.W.M., Alabdulkarem A., Rashed M.M., Teoh Y.H., How H.G. (2016) Higher alcohol–biodiesel–diesel blends: An approach for improving the performance, emission, and combustion of a light-duty diesel engine, *Energy Convers. Manag.* **111**, 174–185. https://doi.org/10.1016/j.enconman.2015.12.066.

35 Zhu L., Xiao Y., Cheung C.S., Guan C., Huang Z. (2016) Combustion, gaseous and particulate emission of a diesel engine fueled with n-pentanol (C5 alcohol) blended with waste cooking oil biodiesel, *Appl. Therm. Eng.* **102**, 73–79. https://doi.org/10.1016/j.applthermaleng.2016.03.145.

36 Yesilyurt M.K., Cesur C. (2022) A statistical optimization attempt by applying the Taguchi technique for the optimum transesterification process parameters in the production of biodiesel from *Papaver somniferum* L. seed oil, *Fuel* **329**, 125406. https://doi.org/10.1016/j.fuel.2022.125406.

37 Krishna S.M., Salam P.A., Tongroon M., Chollacoop N. (2019) Performance and emission assessment of optimally blended biodiesel-diesel-ethanol in diesel engine generator, *Appl. Therm. Eng.* **155**, 525–533. https://doi.org/10.1016/j.applthermaleng.2019.04.012.

38 Elumalai P.V., Dash S.K., Parthasarathy M., Dhineshbabu N.R., Balasubramanian D., Cao D.N., Truong T.H., Le A.T., Hoang A.T. (2022) Combustion and emission behaviors of dual-fuel premixed charge compression ignition engine powered with n-pentanol and blend of diesel/waste tire oil included nanoparticles, *Fuel* **324**, 124603. https://doi.org/10.1016/j.fuel.2022.124603.

39 Ganesan N., Le T.H., Ekambaram P., Balasubramanian D., Hoang A.T. (2022) Experimental assessment on performance and combustion behaviors of reactivity-controlled compression ignition engine operated by n-pentanol and cottonseed biodiesel, *J. Clean. Prod.* **330**, 129781. https://doi.org/10.1016/j.jclepro.2021.129781.

40 Yesilyurt M.K., Eryilmaz T., Arslan M. (2018) A comparative analysis of the engine performance, exhaust emissions and combustion behaviors of a compression ignition engine fuelled with biodiesel/diesel/1-butanol (C4 alcohol) and biodiesel/diesel/n-pentanol (C5 alcohol) fuel blends, *Energy* **165**, 1332–1351. https://doi.org/10.1016/j.energy.2018.10.100.

41 Ashok B., Jeevanantham A.K., Nanthagopal K., Saravanan B., Kumar M.S., Johny A., Abubakar S. (2019) An experimental analysis on the effect of n-pentanol-Calophyllum Inophyllum Biodiesel binary blends in CI engine characteristcis, *Energy* **173**, 290–305. https://doi.org/10.1016/j.energy.2019.02.092.

42 Dincer I., Cengel Y.A. (2001) Energy, entropy and exergy concepts and their roles in thermal engineering, *Entropy* **3**, 3, 116–149. https://doi.org/10.3390/e3030116.

43 Sarıkoç S., Örs İ., Ünalan S. (2020) An experimental study on energy-exergy analysis and sustainability index in a diesel engine with direct injection diesel-biodiesel-butanol fuel blends, *Fuel* **268**, 117321. https://doi.org/10.1016/j.fuel.2020.117321.

44 Şanli B.G., Uludamar E., Özcanli M. (2019) Evaluation of energetic-exergetic and sustainability parameters of biodiesel fuels produced from palm oil and opium poppy oil as alternative fuels in diesel engines, *Fuel* **258**, 116116. https://doi.org/10.1016/j.fuel.2019.116116.

45 Yaman H. (2022) Investigation of the effect of compression ratio on the energetic and exergetic performance of a CI engine operating with safflower oil methyl ester, *Process Saf. Environ. Prot.* **158**, 607–624. https://doi.org/10.1016/j.psep.2021.12.014.

46 Aghbashlo M., Tabatabaei M., Mohammadi P., Pourvosoughi N., Nikbakht A.M., Goli S.A.H. (2015) Improving exergetic and sustainability parameters of a DI diesel engine using polymer waste dissolved in biodiesel as a novel diesel additive, *Energy Convers. Manag.* **105**, 328–337. https://doi.org/10.1016/j.enconman.2015.07.075.

47 Panigrahi N., Mohanty M.K., Mishra S.R., Mohanty R.C. (2014) Performance, emission, energy, and exergy analysis of a CI engine using mahua biodiesel blends with diesel, *Int. Sch. Res. Notices* **2014**, 207465. https://doi.org/10.1155/2014/207465.

48 Tat M.E. (2011) Cetane number effect on the energetic and exergetic efficiency of a diesel engine fuelled with biodiesel, *Fuel Process. Technol.* **92**, 7, 1311–1321. https://doi.org/10.1016/j.fuproc.2011.02.006.

49 Chaudhary V., Gakkhar R. (2020) Exergy based performance comparison of DI diesel engine fuelled with WCO15 and NEEM15 biodiesel, *Environ. Prog. Sustain. Energy* **39**, 3, e13363. https://doi.org/10.1002/ep.13363.

50 Sayin Kul B., Kahraman A. (2016) Energy and exergy analyses of a diesel engine fuelled with biodiesel-diesel blends containing 5% bioethanol, *Entropy* **18**, 11, 387. https://doi.org/10.3390/e18110387.

51 Dincer I. (2000) Thermodynamics, exergy and environmental impact, *Energy Sources* **22**, 8, 723–732. https://doi.org/10.1080/00908310050120272.

52 Canakci M., Hosoz M. (2006) Energy and exergy analyses of a diesel engine fuelled with various biodiesels, *Energy Sources Part B* **1**, 4, 379–394. https://doi.org/10.1080/15567240500400796.

53 Ağbulut Ü. (2022) Understanding the role of nanoparticle size on energy, exergy, thermoeconomic, exergoeconomic, and sustainability analyses of an IC engine: A thermodynamic approach, *Fuel Process. Technol.* **225**, 107060. https://doi.org/10.1016/j.fuproc.2021.107060.

54 Tiwari C., Verma T.N., Dwivedi G., Verma P. (2023) Energy-exergy analysis of diesel engine fueled with microalgae biodiesel-diesel blend, *Appl. Sci.* **13**, 3, 1857. https://doi.org/10.3390/app13031857.

55 Caliskan H., Tat M.E., Hepbasli A. (2009) Performance assessment of an internal combustion engine at varying dead (reference) state temperatures, *Appl. Therm. Eng.* **29**, 16, 3431–3436. https://doi.org/10.1016/j.applthermaleng.2009.05.021.

56 Rangasamy M., Duraisamy G., Govindan N. (2020) A comprehensive parametric, energy and exergy analysis for oxygenated biofuels based dual-fuel combustion in an automotive light duty diesel engine, *Fuel* **277**, 118167. https://doi.org/10.1016/j.fuel.2020.118167.

57 Kavitha K.R., Jayaprabakar J., Prabhu A. (2022) Exergy and energy analyses on biodiesel–diesel-ethanol blends in a diesel engine, *Int. J. Ambient Energy* **43**, 1, 778–782. https://doi.org/10.1080/01430750.2019.1670261.

58 Çalışkan H. (2020) Energy, exergy, thermoecologic, sustainability, thermoeconomic and exergoeconomic analyses of solar collectors, *Eng. Mach.* **61**, 700, 228–240. https://doi.org/10.46399/muhendismakina.774277. (in Turkish)

59 Sekmen P., Yılbaşı Z. (2011) Application of energy and exergy analyses to a CI engine using biodiesel fuel, *Math. Comput. Appl.* **16**, 4, 797–808. https://doi.org/10.3390/mca16040797.

60 Kaya C., Aydin Z., Kökkülünk G., Safa A. (2020) Exergetic and exergoeconomic analyzes of compressed natural gas as an alternative fuel for a diesel engine, *Energy Sources Part A* **45**, 2, 3722–3741. https://doi.org/10.1080/15567036.2020.1811429.

61 Murugapoopathi S., Vasudevan D. (2019) Energy and exergy analysis on variable compression ratio multi-fuel engine, *J. Therm. Anal. Calorim.* **136**, 255–266. https://doi.org/10.1007/s10973-018-7761-2.

62 Hoseinpour M., Sadrnia H., Tabasizadeh M., Ghobadian B. (2017) Energy and exergy analyses of a diesel engine fueled with diesel, biodiesel-diesel blend and gasoline fumigation, *Energy* **141**, 2408–2420. https://doi.org/10.1016/j.energy.2017.11.131.

63 Reşitoğlu İ.A., Altinişik K., Keskin A. (2015) The pollutant emissions from diesel-engine vehicles and exhaust after treatment systems, *Clean Technol. Environ. Policy* **17**, 15–27. https://doi.org/10.1007/s10098-014-0793-9.

64 Sekmen Y., Çınar C., Erduranlı P., Boran E. (2004) The investigation of the effect of injection pressure and maximum fuel quantity on engine performance and smoke emissions in diesel engines, *J. Polytech.* **7**, 4, 321–326.

65 Açıkkalp E., Aras H., Hepbasli A. (2014) Advanced exergoeconomic analysis of a trigeneration system using a diesel-gas engine, *Appl. Therm. Eng.* **67**, 1–2, 388–395. https://doi.org/10.1016/j.applthermaleng.2014.03.005.

66 Yildirim U., Gungor A. (2012) An application of exergoeconomic analysis for a CHP system, *Int. J. Electr. Power Energy Syst.* **42**, 1, 250–256. https://doi.org/10.1016/j.ijepes.2012.03.040.

67 Uysal C., Ağbulut Ü., Elibol E., Demirci T., Karagoz M., Saridemir S. (2022) Exergetic, exergoeconomic, and sustainability analyses of diesel–biodiesel fuel blends including synthesized graphene oxide nanoparticles, *Fuel* **327**, 125167. https://doi.org/10.1016/j.fuel.2022.125167.